

MORPHOLOGICAL SHAPE DECOMPOSITION



SPOT data of Machap Baru catchment and its surroundings



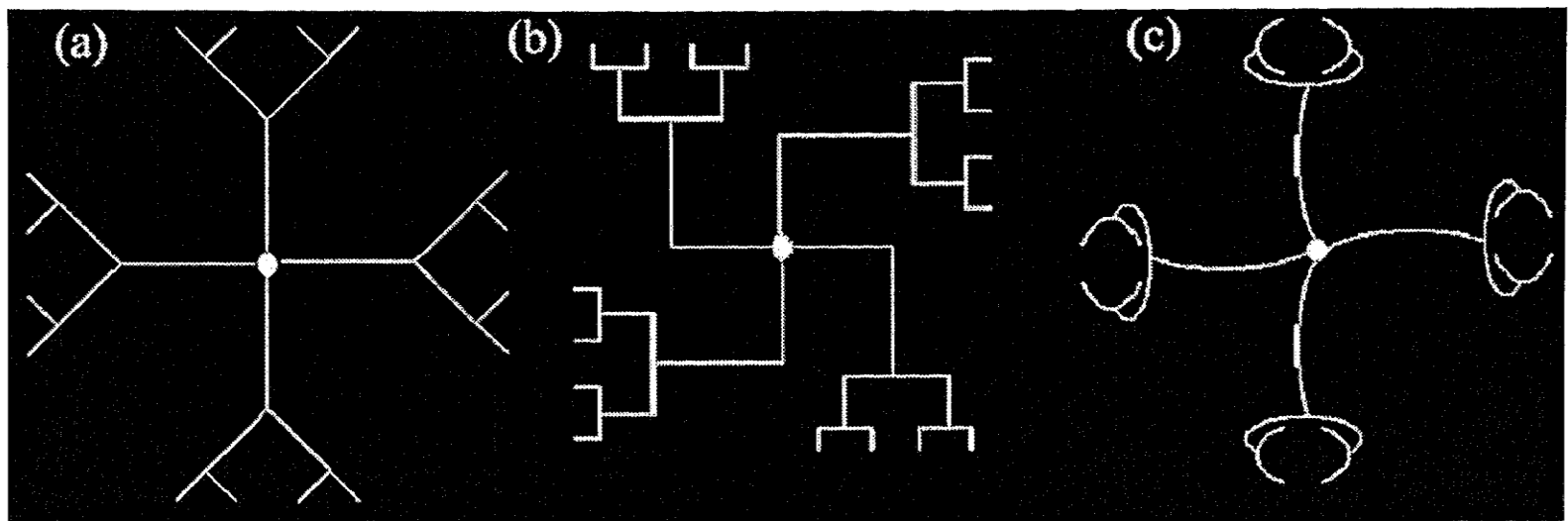
Machap Baru reservoir catchment area

Scale Invariant But Shape
Dependent Power-laws

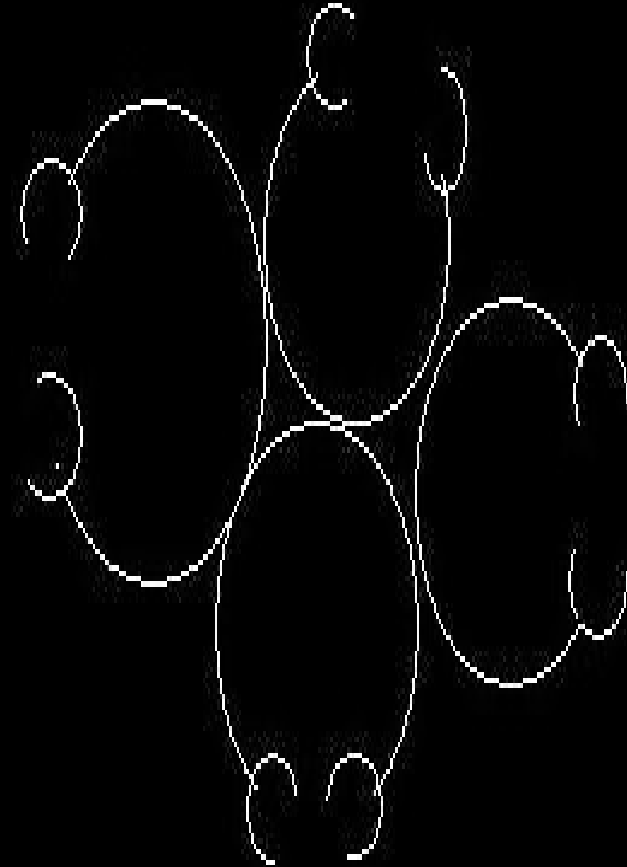
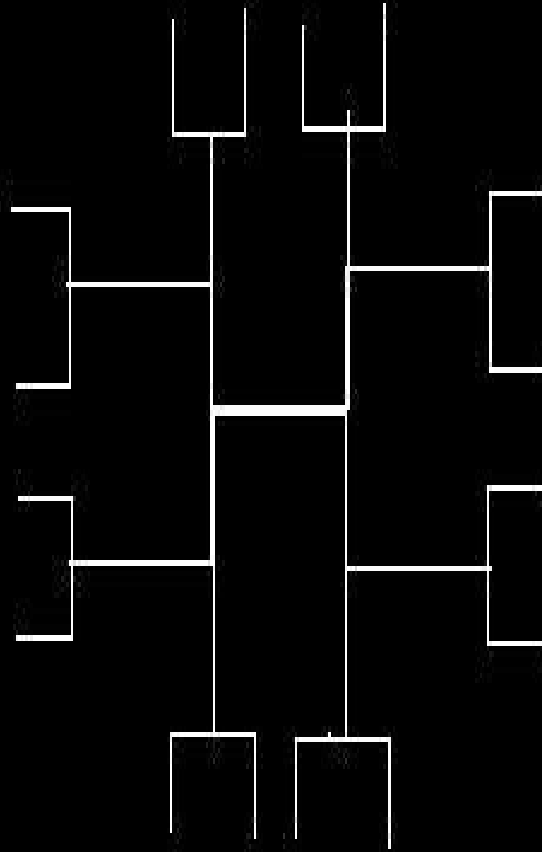
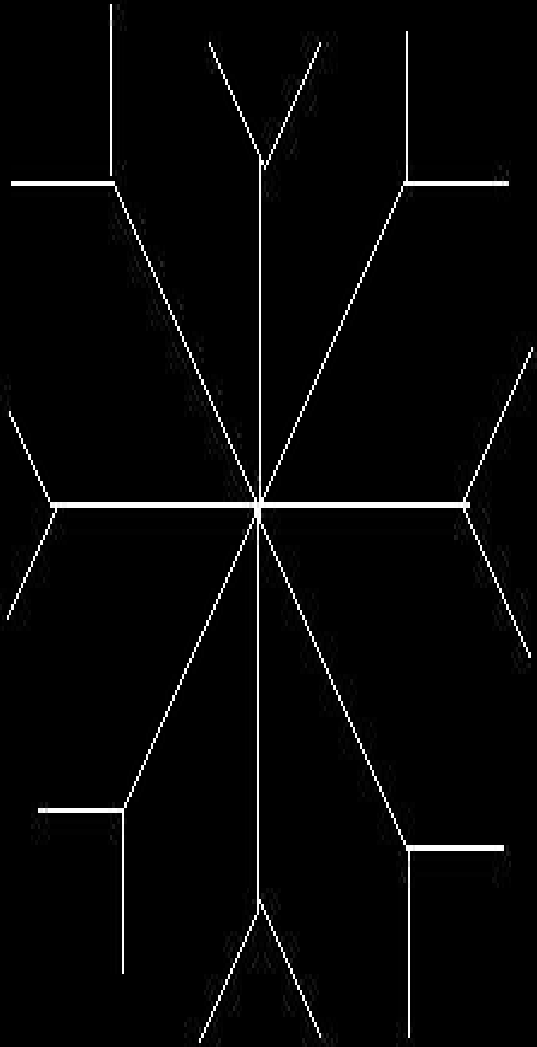
Objectives

To propose morphology based method via fragmentation rules to compute scale invariant but shape-dependent measures of non-network space of a basin.

To make comparisons between morphometry based parameters / dimensions and dimensions derived for non-network space.



Topologically Invariant networks with variant geometric organization



Schematically represented networks

Proposed Technique

Step1: Channel network is traced from topographic map.

Step2: Channel network is dilated and eroded iteratively until the entire basin is filled up with white space. This step is to generate catchment boundary automatically. Dilation followed by erosion is called structural closing, which will smoothen the image.

Step3: Generate the basin with channel network and non-network space with boundary by subtracting the channel network from the catchment boundary achieved in Step2.

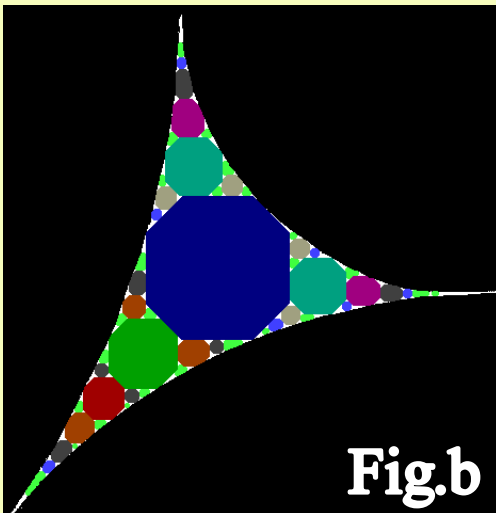
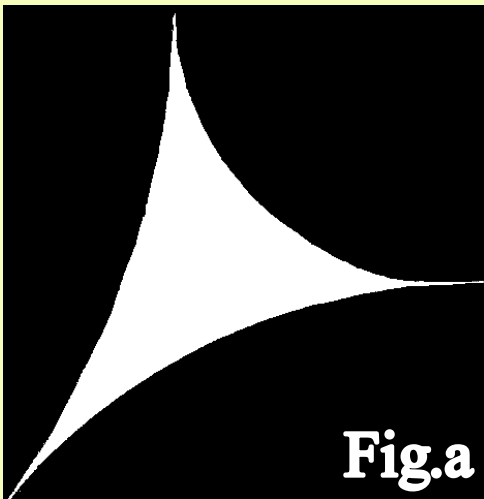
Step4: Structural opening (erosion followed by dilation) is performed recursively in basin achieved in Step3 to fill the entire basin of non-network space with varying size of octagons.

Step5: Assign unique color for each size of octagons.

Step6: Compute morphometry for the basin.

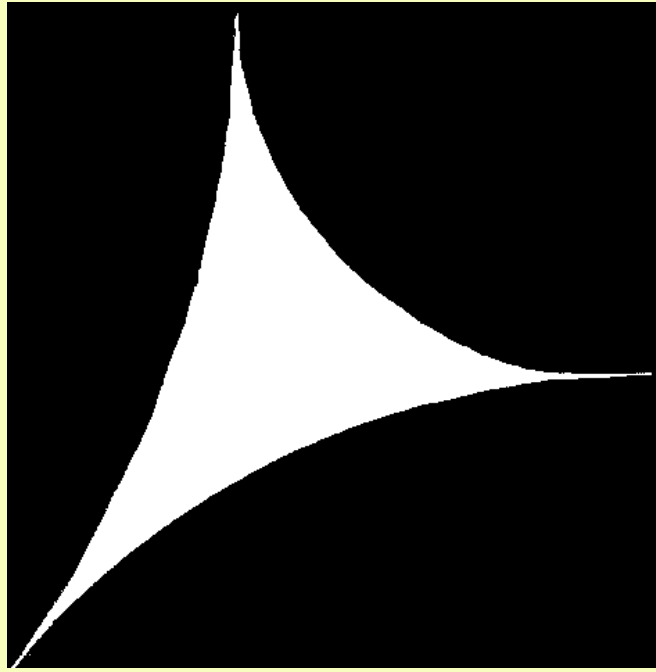
Step7: Compute shape dependent dimension.

Power law relationship

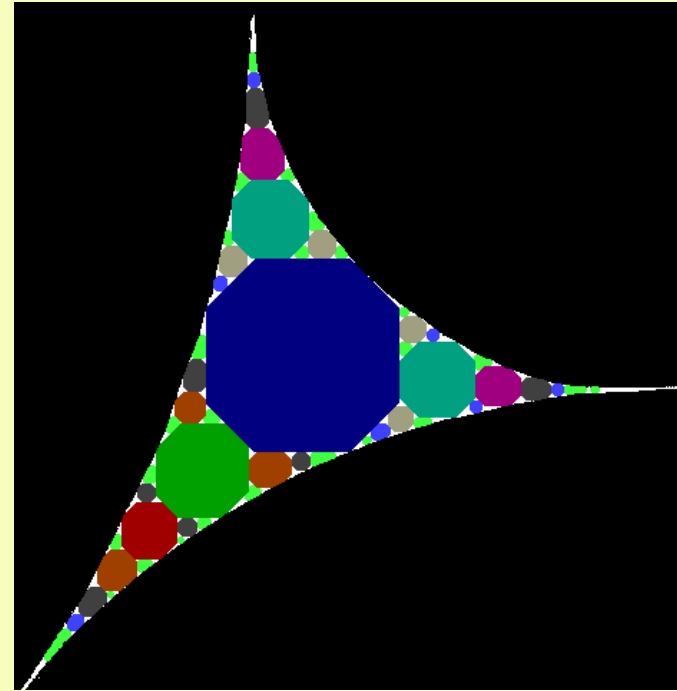


- As per the previous fig. the slopes of the best-fit lines (α_N and α_A) for number-radius and area-radius relationships yield 2.37 and 1.34.
- These slope values of the best-fit lines provide shape dependent dimensions as $D_N = \alpha_N - 1$ and $D_A = \alpha_A$.
- As in previous Fig., D_N and D_A for non-network space yield 1.37 and 1.34.
- A Power-law relationship is shown in earlier Fig. with an exponent value 1.79 between the area and number of NODs observed with increasing radius of structuring template.

(a) Apollonian Space, and (b) after decomposition by means of octagon.



(a)

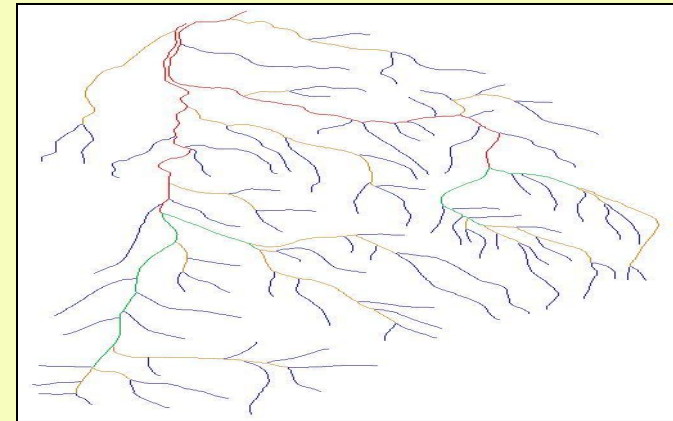


(b)

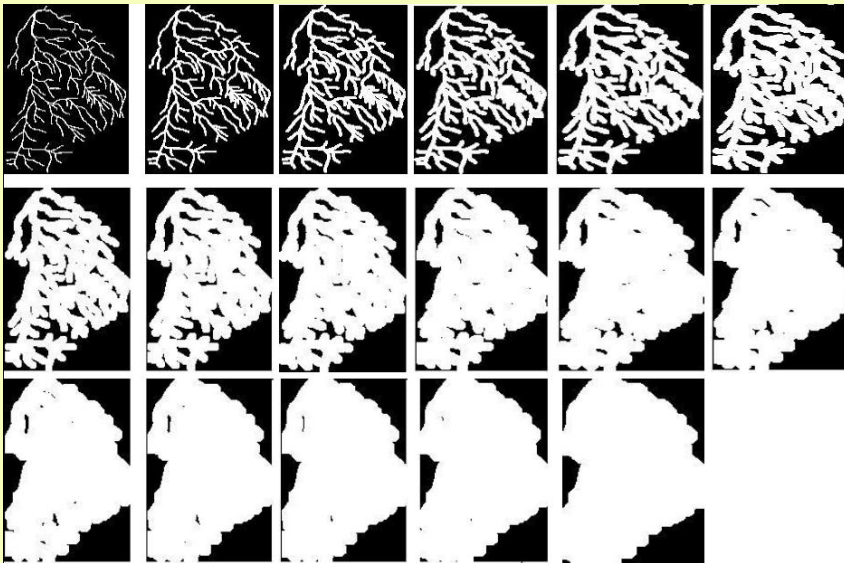
(a) Appollonian Space, and (b) after decomposition by means of octagon.

Algorithm Implementation:

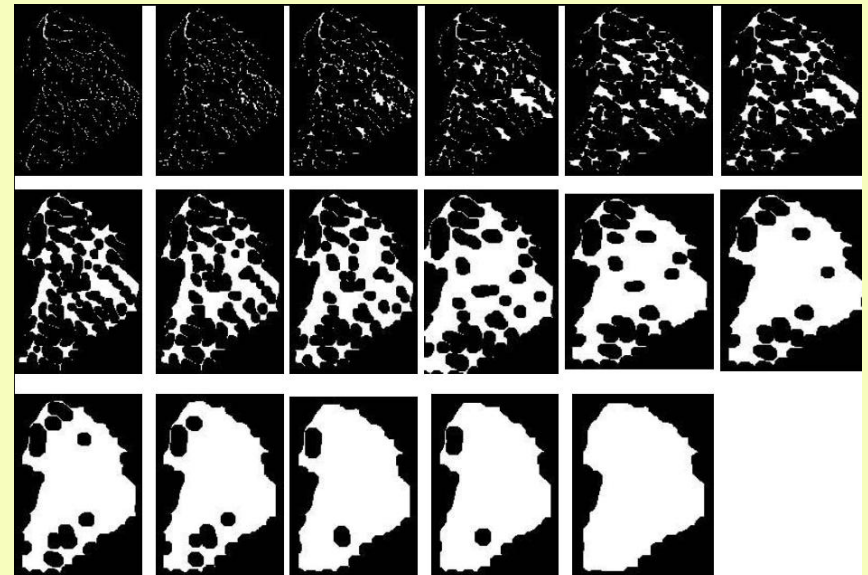
Step 1: **Channel network of sub basin 1**



Step 2: **Close-Hull Generation**



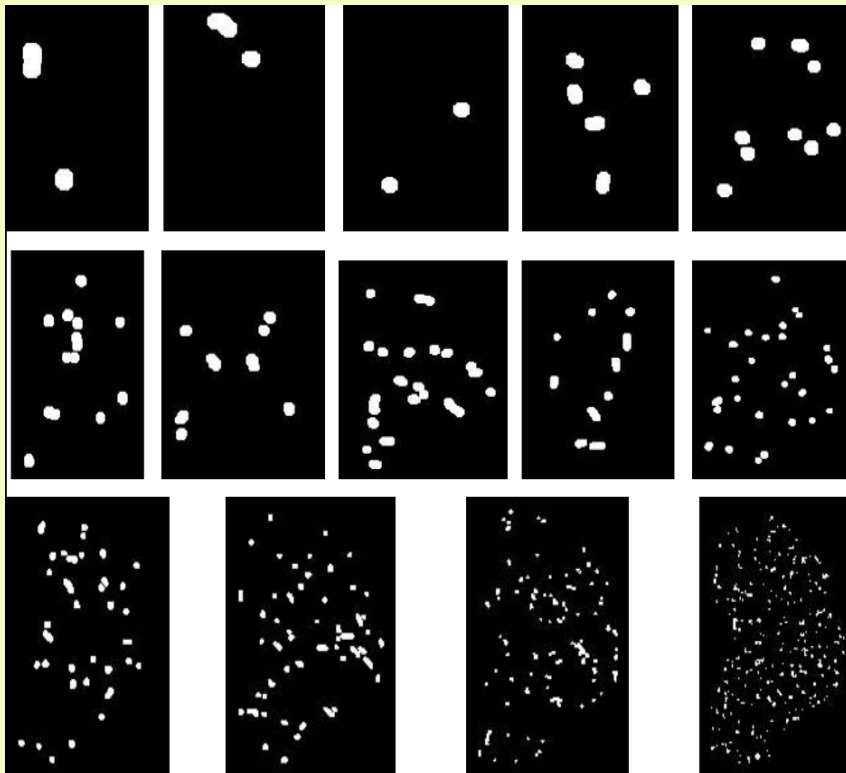
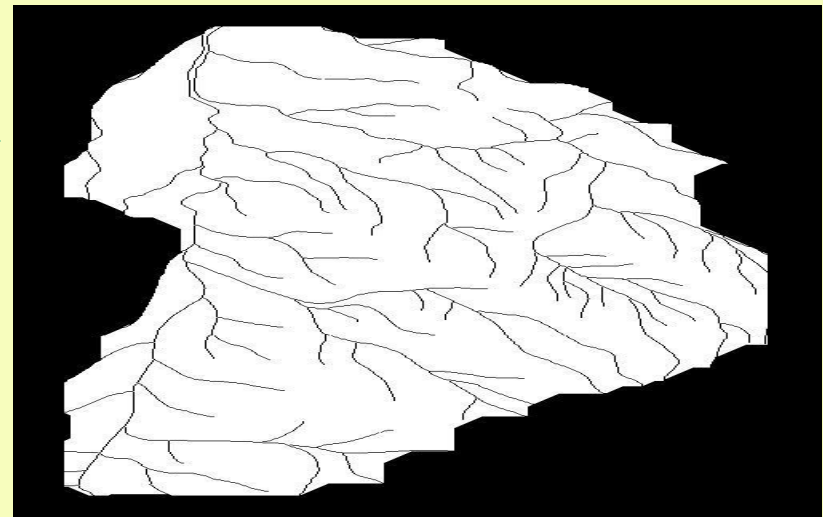
Iterative dilation of channel network of basin 1



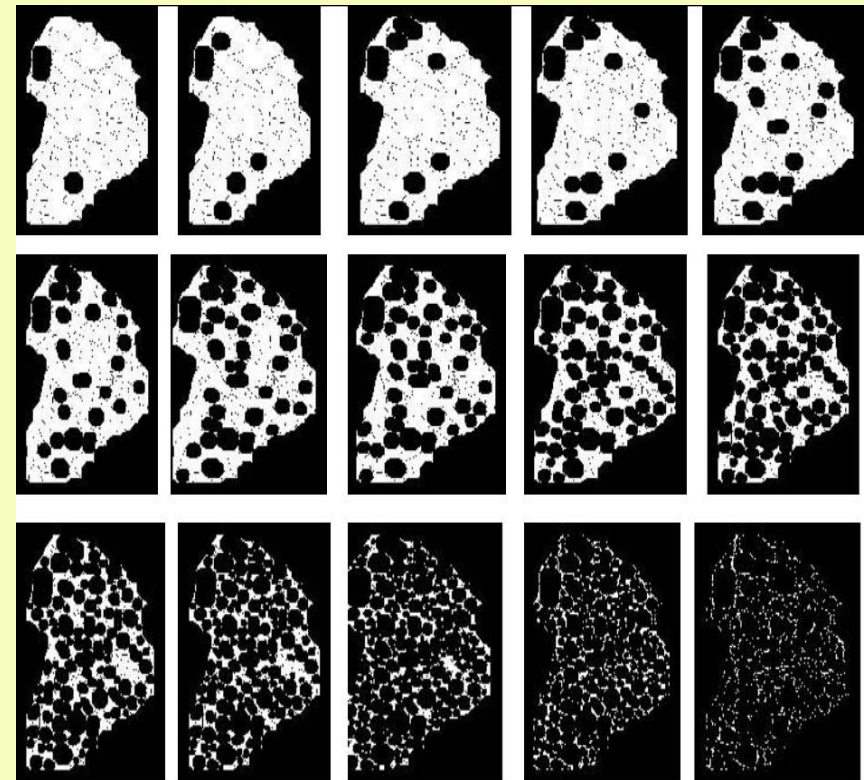
Iterative erosion applied to previous Fig

Step 3: Non-network space
of basin 1

Iterative erosion applied to
step-3 Fig.

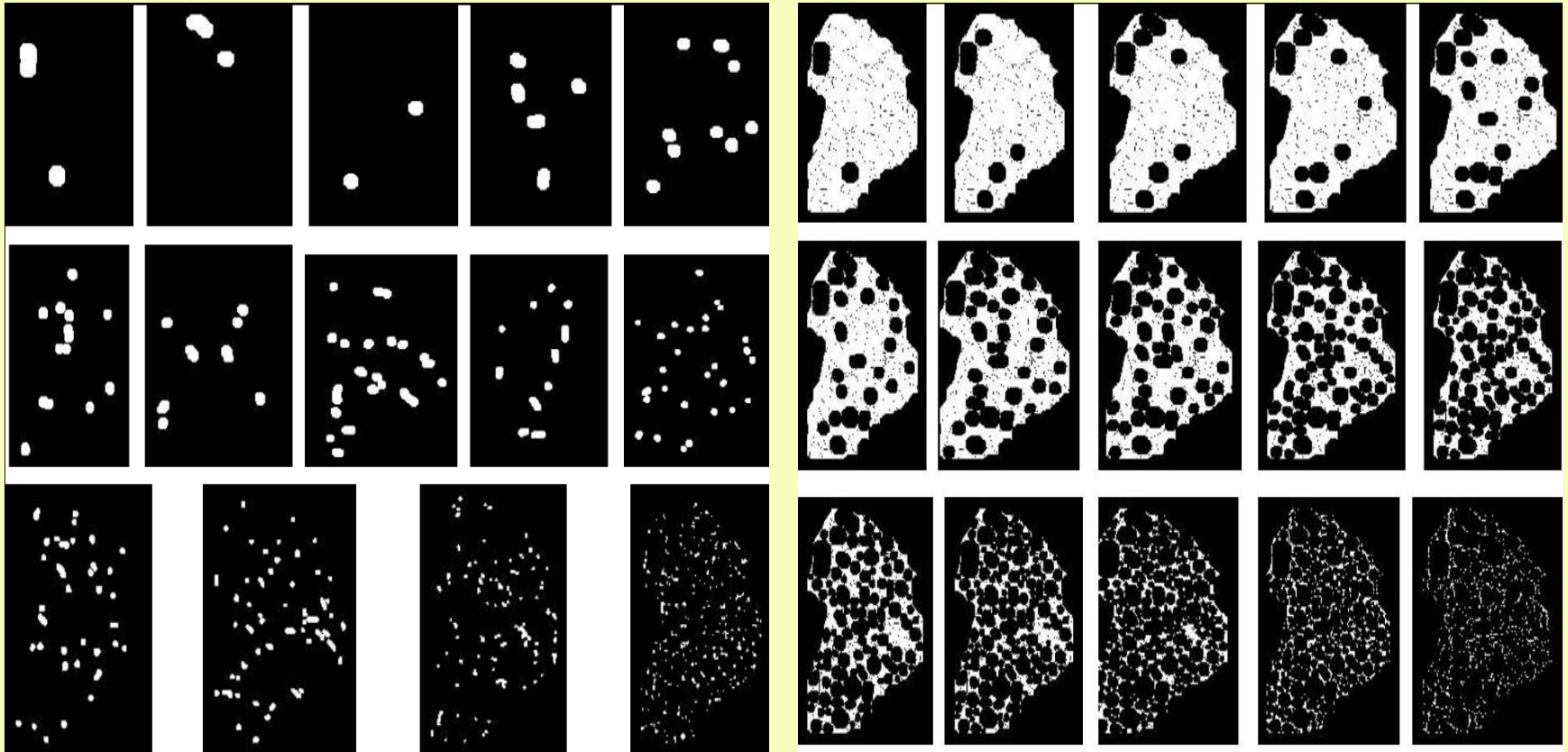


Iterative erosion applied to previous Fig.



Iterative dilation applied to previous Fig.

Step 4: Non-Network Space Decomposition

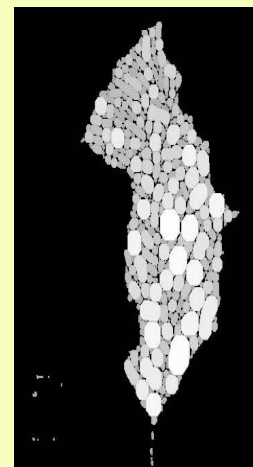
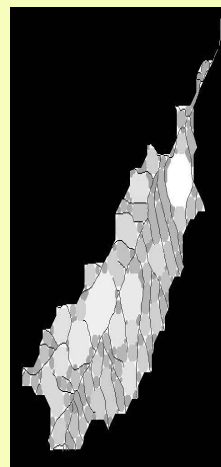
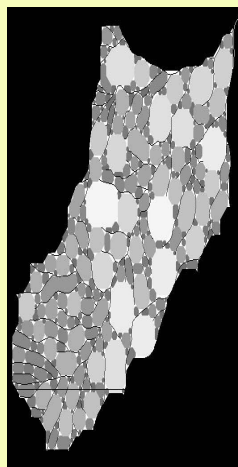
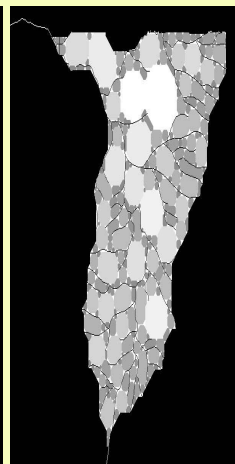
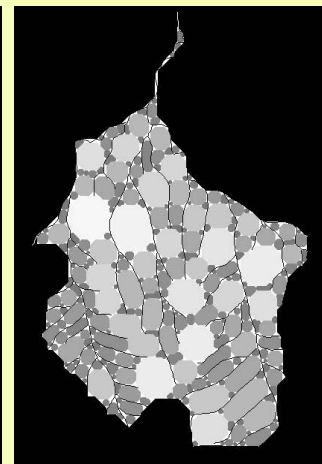
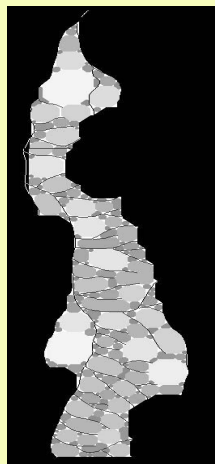
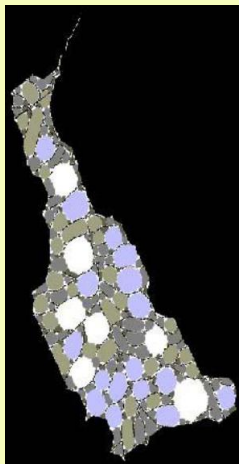
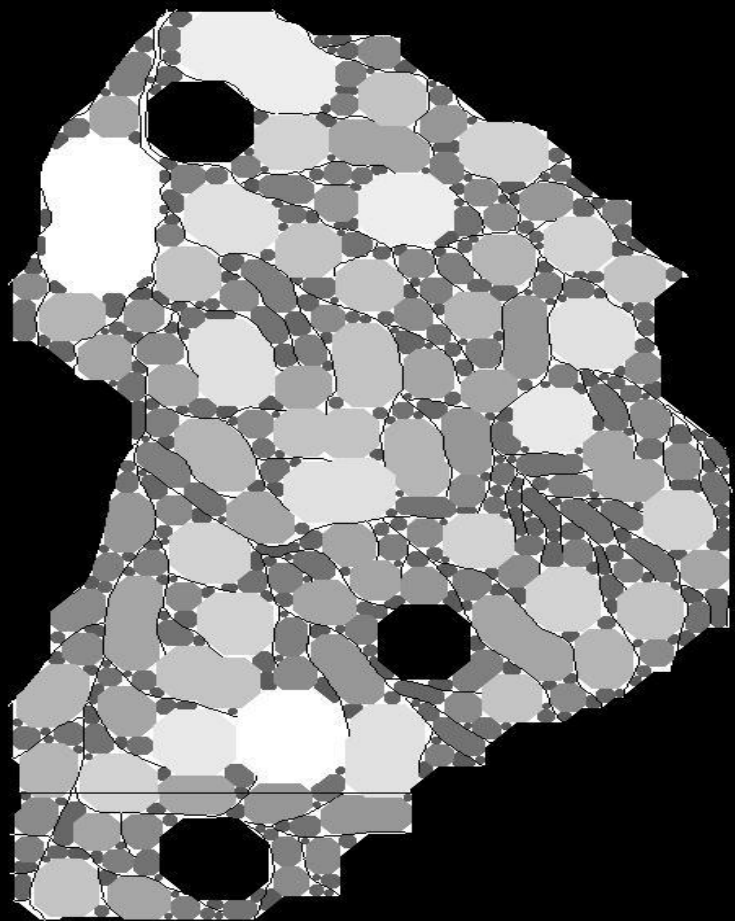


Iterative erosion applied to previous Fig.

Iterative dilation applied to previous Fig.

Decomposition of Non-network space in to non-overlapping disks of octagon shape of several sizes for basin 1

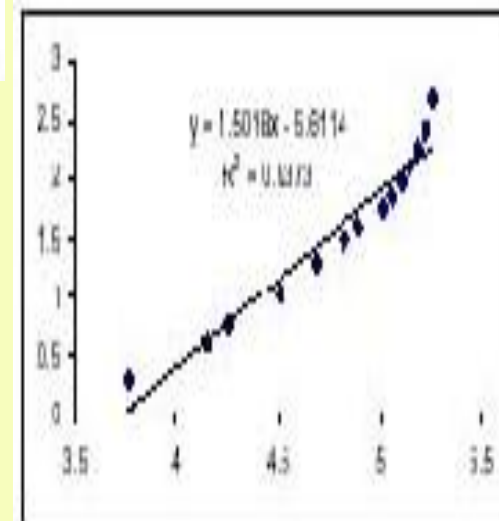
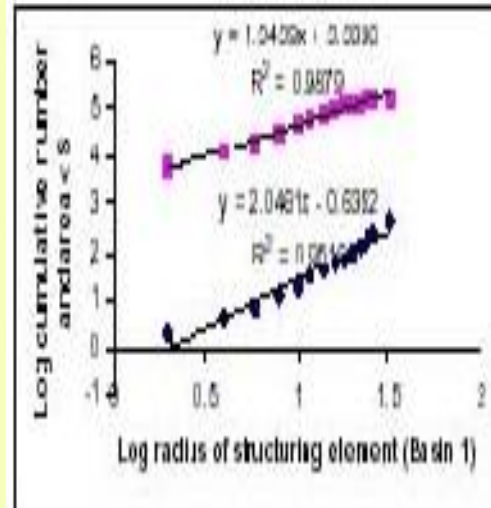
Non-Network Spaces Packed with Non-Overlapping Disks of basins 2 to 8



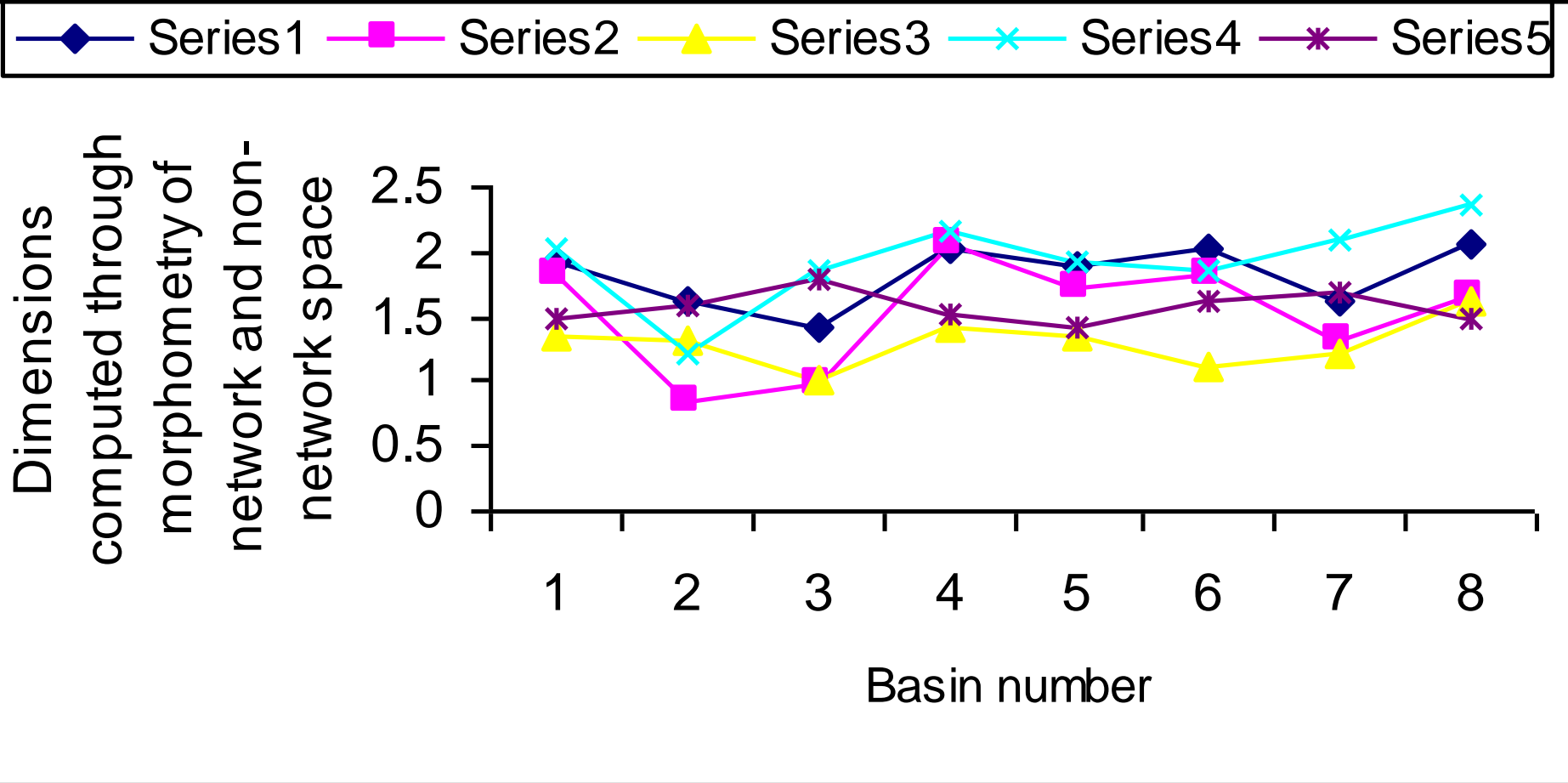
Dimensions derived from morphometry of network and non network space

Morphometric parameter computations achieved through decomposition of non-network space

Basin n#	Network FD	Log Rs/ Log RN	R vs A	R vs N	A vs N
1	1.83	1.93	1.34	2.06	1.50
2	0.86	1.63	1.33	1.23	1.59
3	0.98	1.41	1.02	1.87	1.80
4	2.07	2.01	1.43	2.17	1.52
5	1.73	1.90	1.34	1.94	1.43
6	1.84	2.04	1.13	1.87	1.63
7	1.33	1.61	1.23	2.08	1.70
8	1.65	2.06	1.61	2.38	1.49



Basin number versus varied dimensions derived from morphometry of networks and non-network spaces



Fractal dimension of non-network space of a catchment basin

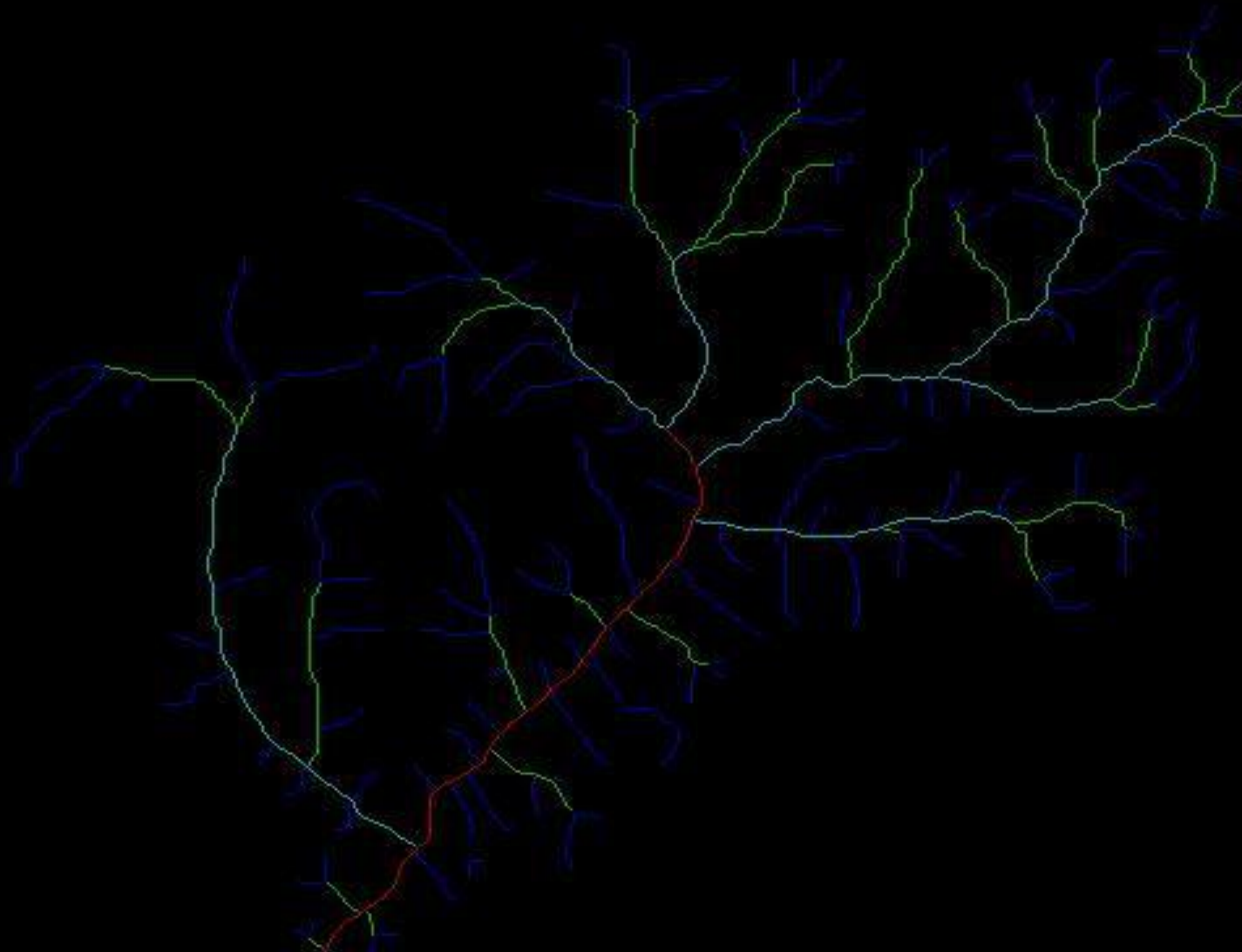
- ◆ **Data used:** Stream network of Machap Baru catchment basin traced from topographic map.
- ◆ **Non-network space:** It is similar to the space that is achieved by subtracting channelized portions from the watershed space.
- ◆ A technique proposed (i) to generate non-network space of a catchment basin, and (ii) to compute an alternative shape dependent quantity like fractal dimension to characterize the non-network space.

Proposed Technique

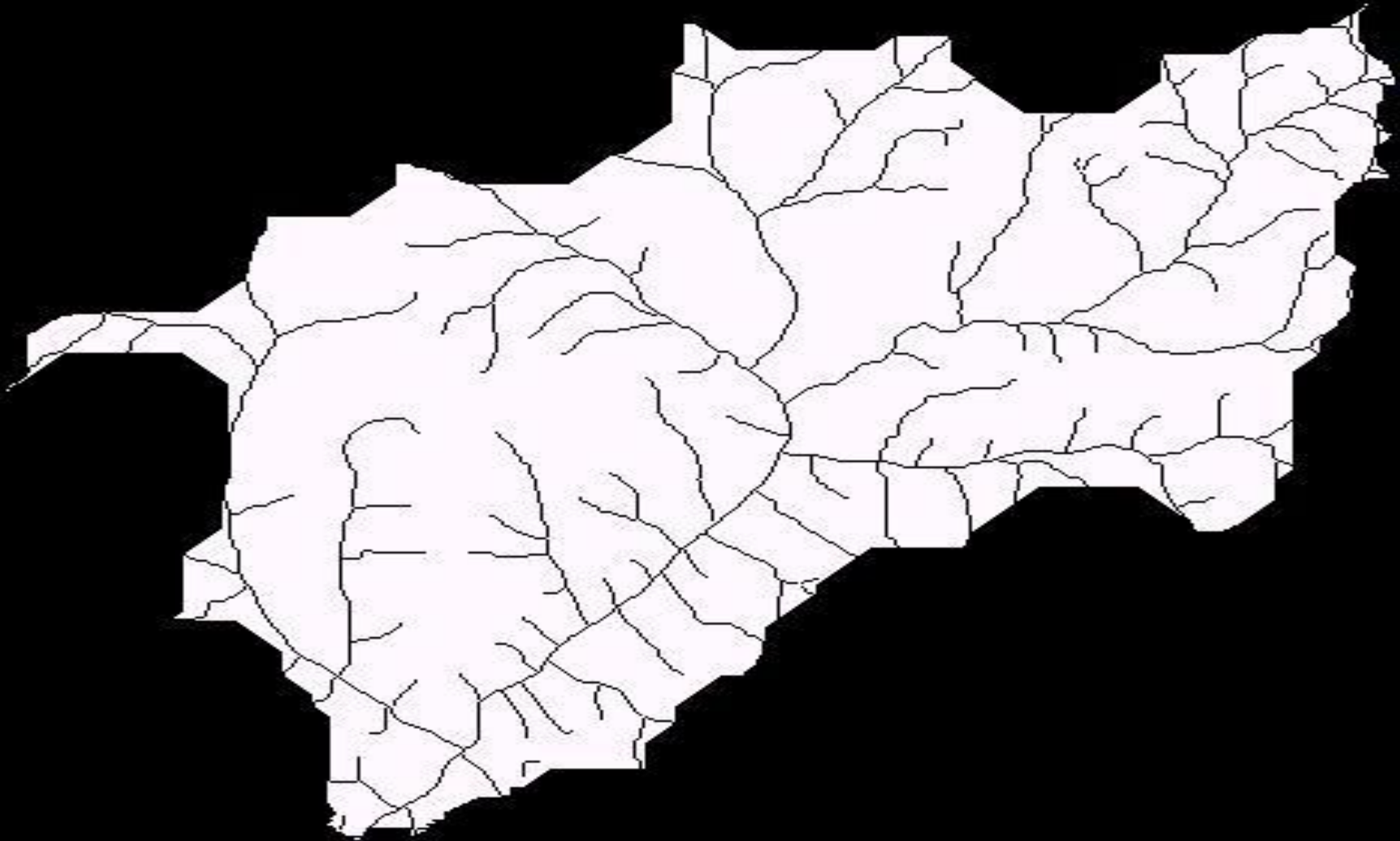
- ◆ Step1: Channel network is traced from topographic map.
- ◆ Step2: Channel network is dilated and eroded iteratively until the entire basin is filled up with white space. This step is to generate catchment boundary automatically. Dilation followed by erosion is called structural closing, which will smoothen the image.
- ◆ Step3: Generate the basin with channel network and non-network space with boundary by subtracting the channel network from the catchment boundary achieved in Step2.

Proposed Technique

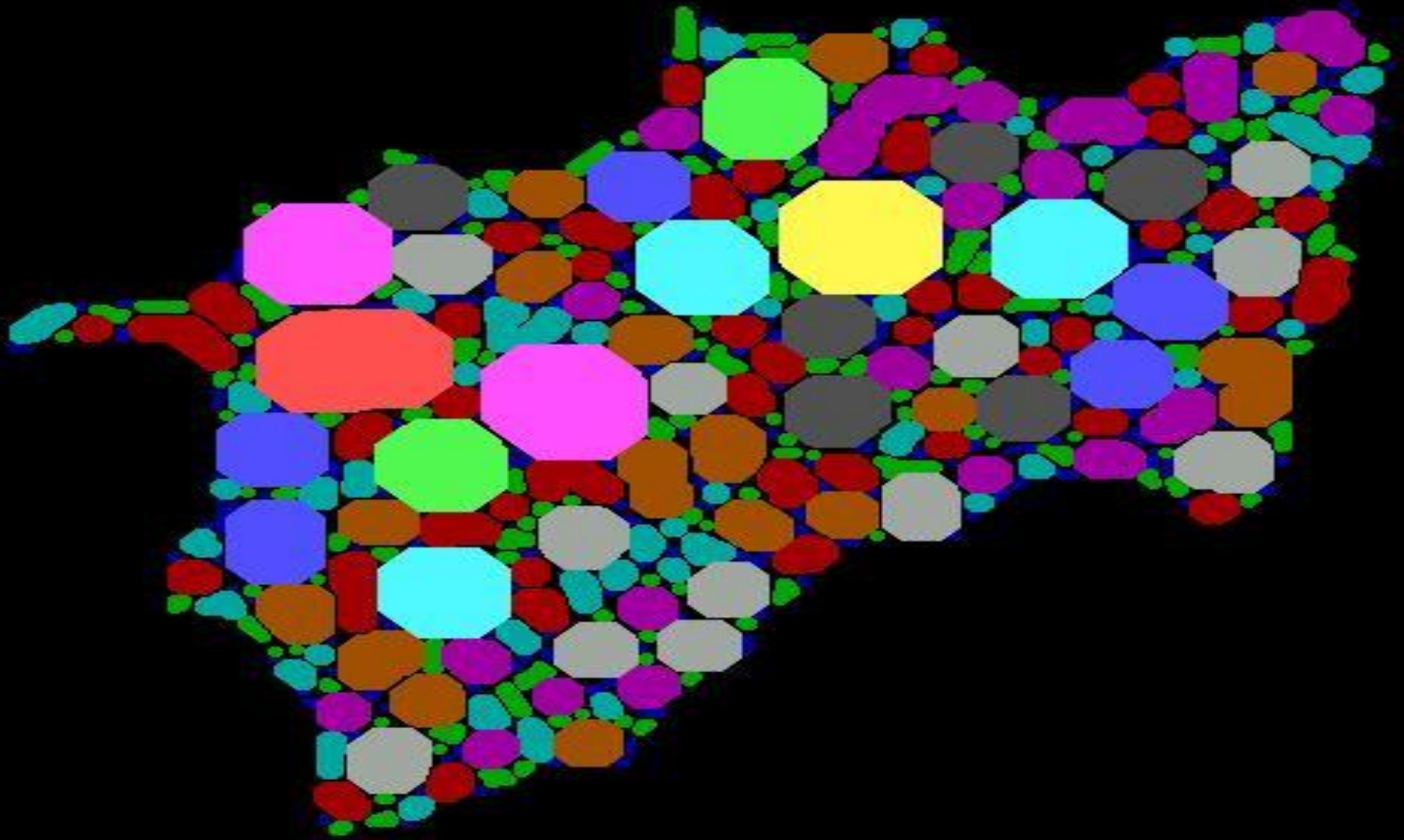
- ◆ Step4: Structural opening (erosion followed by dilation) is performed recursively in basin achieved in Step3 to fill the entire basin of non-network space with varying size of octagons.
- ◆ Step5: Assign unique color for each size of octagons.
- ◆ Step6: Compute morphometry for the basin.
- ◆ Step7: Compute shape dependent dimension.



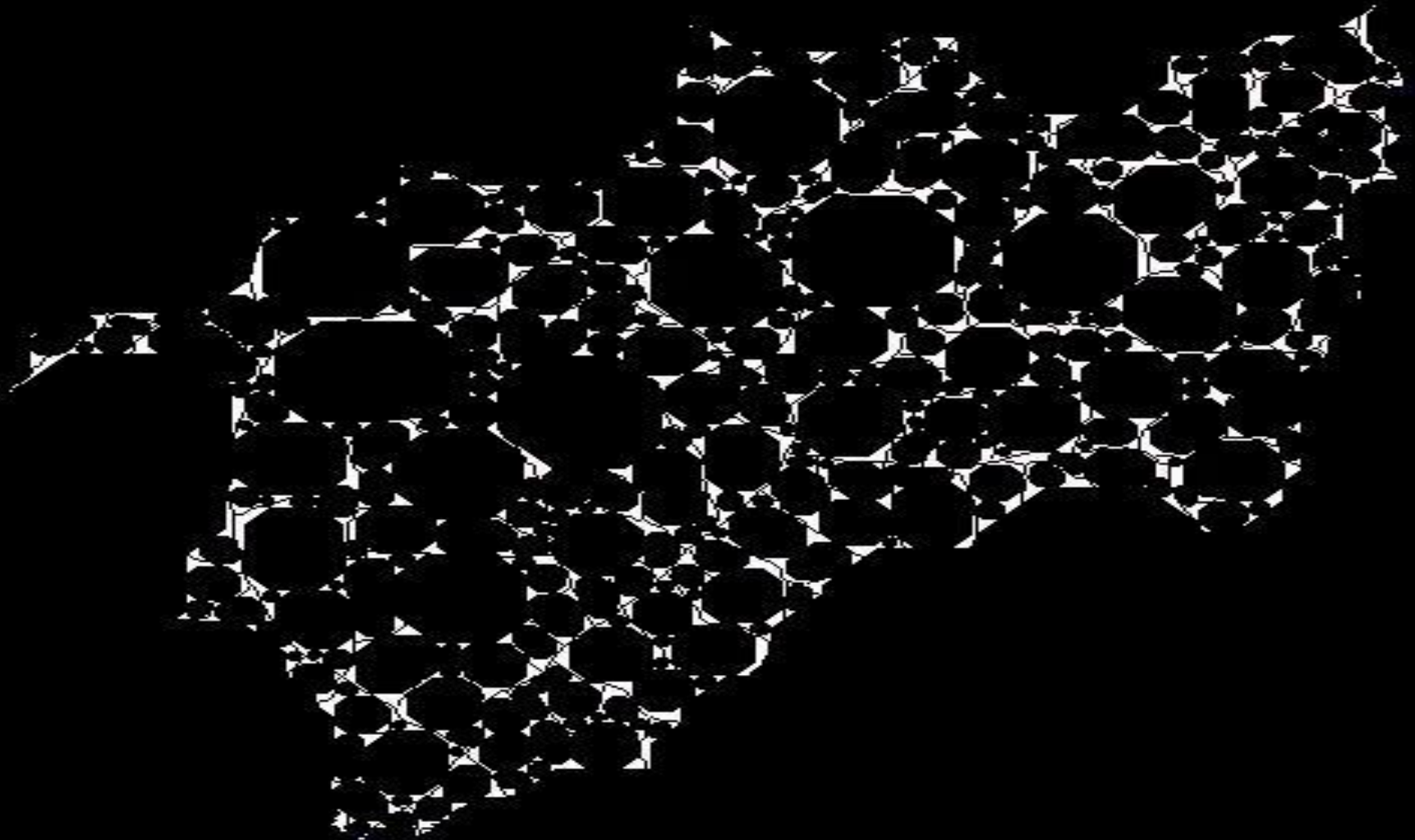
Channel network of Machap Baru reservoir



Non-network space within Catchment basin



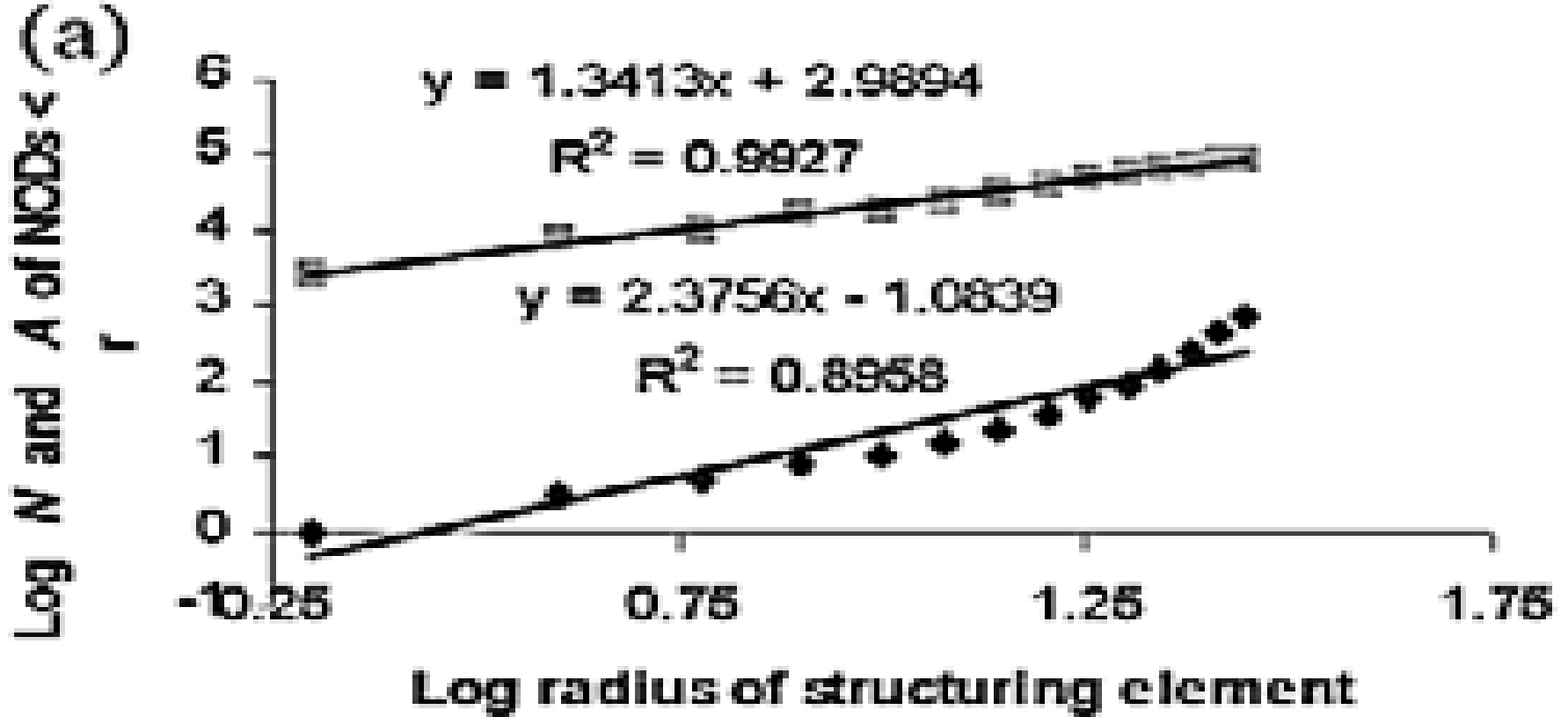
Decomposition of Non-network space in to
non-overlapping disks of octagon shape of
several sizes



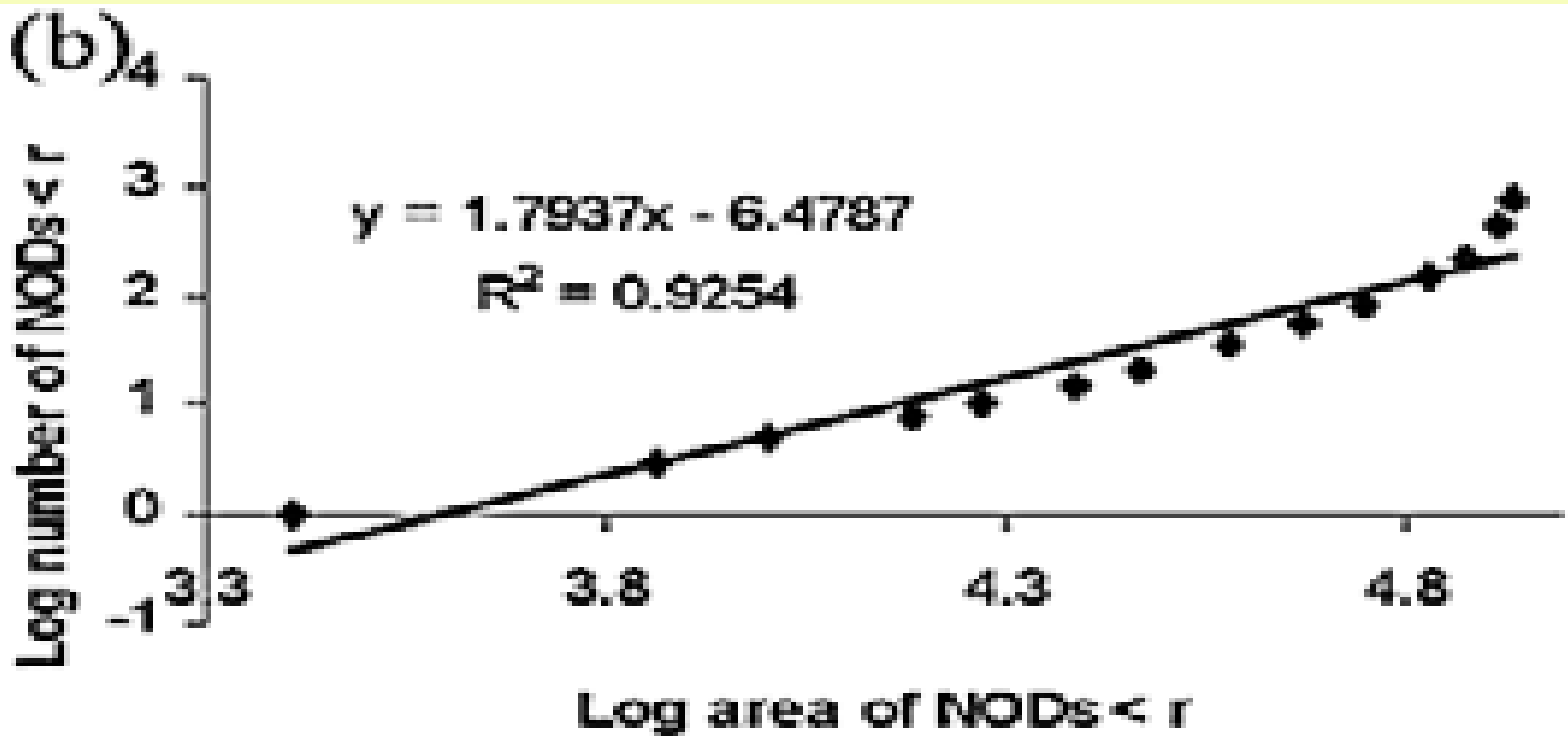
Transition lines between the packed objects

Morphometry and shape dependent dimension computation

- ◆ The ratio of logarithms of bifurcation and mean length ratios of the network yields fractal dimension of 1.77.
- ◆ Power law exponent is determined for NOD's number and size distributions.
- ◆ Number of NODs smaller than the specified threshold radius of structuring template and their contributing areas are computed.
- ◆ Simple Power law relationship is derived by employing these numbers, their contributing areas and the corresponding radius of template.



Double logarithmic plot between radii of structuring templates and corresponding number and area of NODs



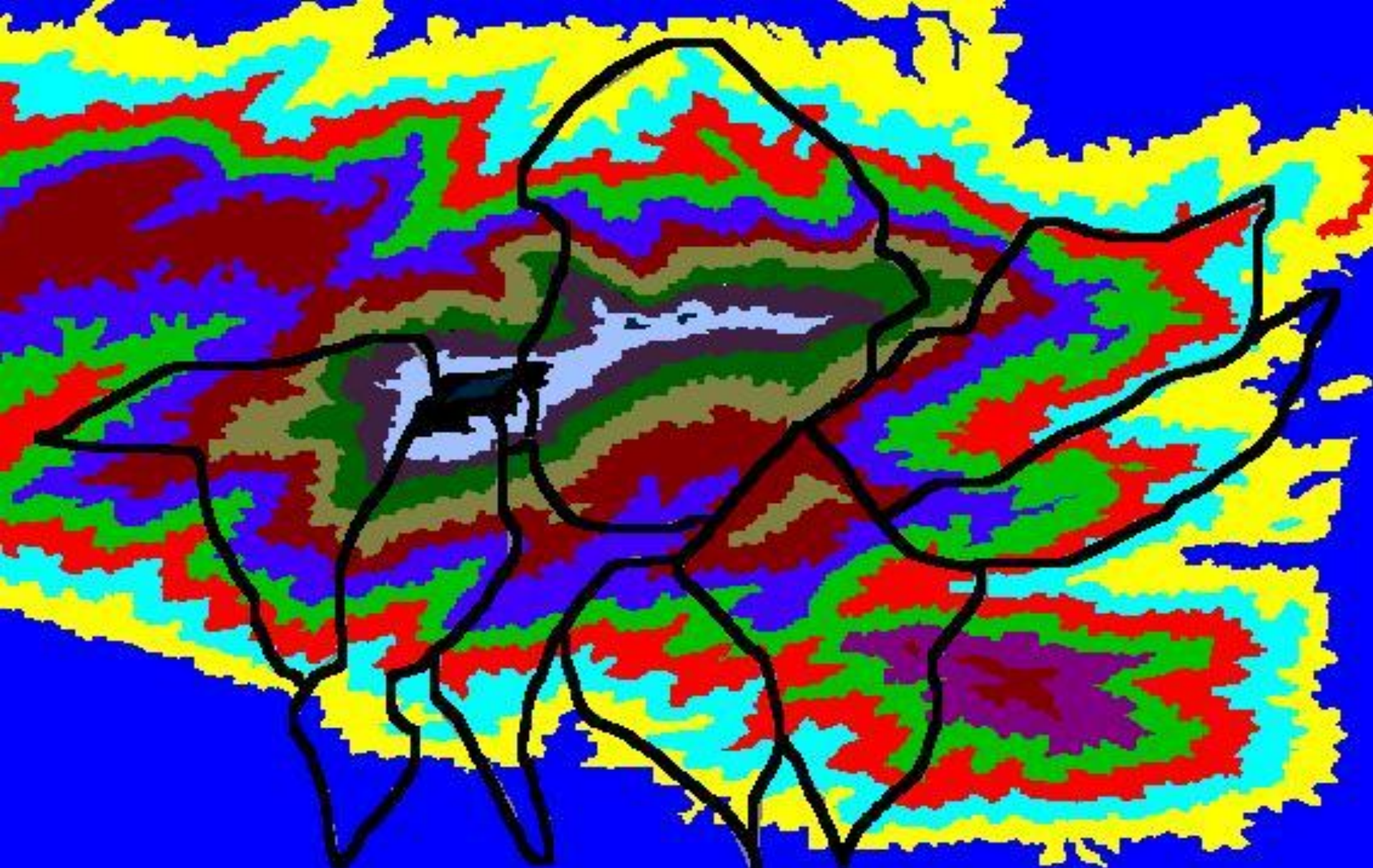
Double logarithmic plot between area and number of NOD's with increasing radius of structuring element

Power law relationship

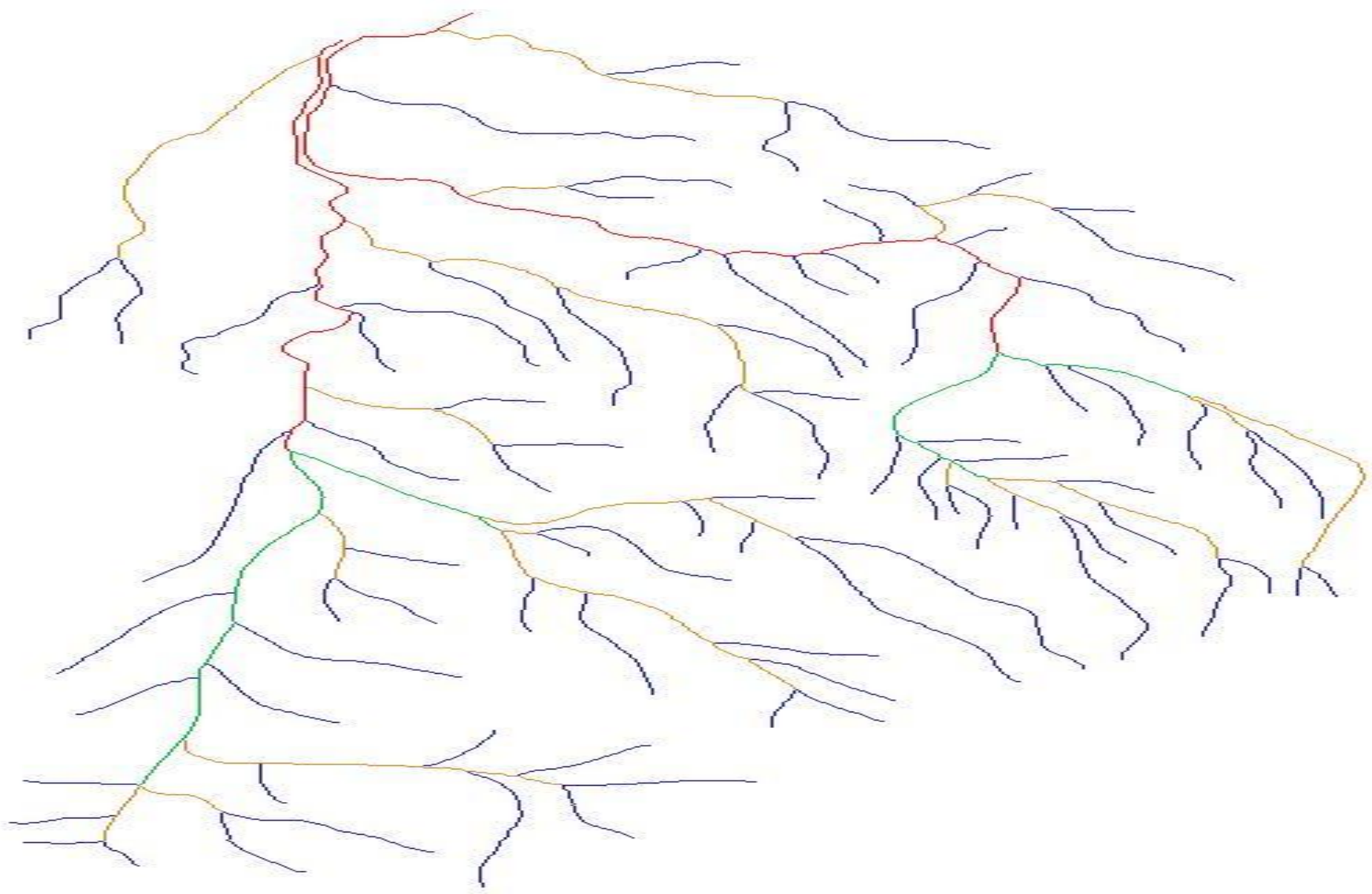
- ◆ As in previous Fig., the slopes of the best-fit lines (α_N and α_A) for number-radius and area-radius relationships yield 2.37 and 1.34.
- ◆ These slope values of the best-fit lines provide shape dependent dimensions as $D_N = \alpha_N - 1$ and $D_A = \alpha_A$.
- ◆ As in previous Fig., D_N and D_A for non-network space yield 1.37 and 1.34.
- ◆ A Power-law relationship is shown in earlier Fig. with an exponent value 1.79 between the area and number of NODs observed with increasing radius of structuring template

Morphometry of Network and Non-Network space

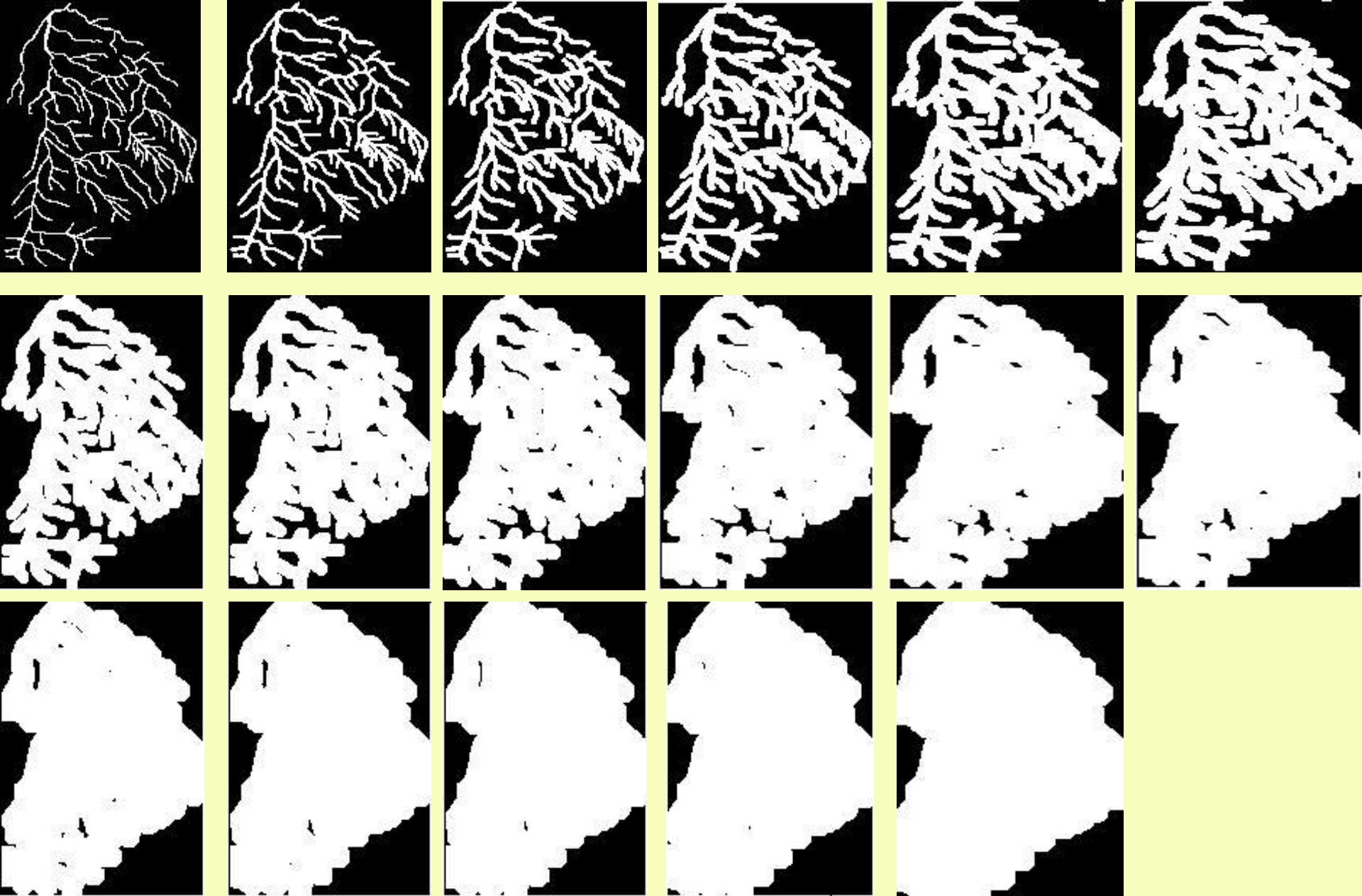
- ◆ **Data Used:** Digital Elevation Model of Gunung Ledang region.
- ◆ This technique is adopted to generate non-network space of eight sub-basins of Gunung Ledang region.
- ◆ In this phase, relationships between the dimensions estimated via morphometries of the network and their corresponding non-network spaces is shown.



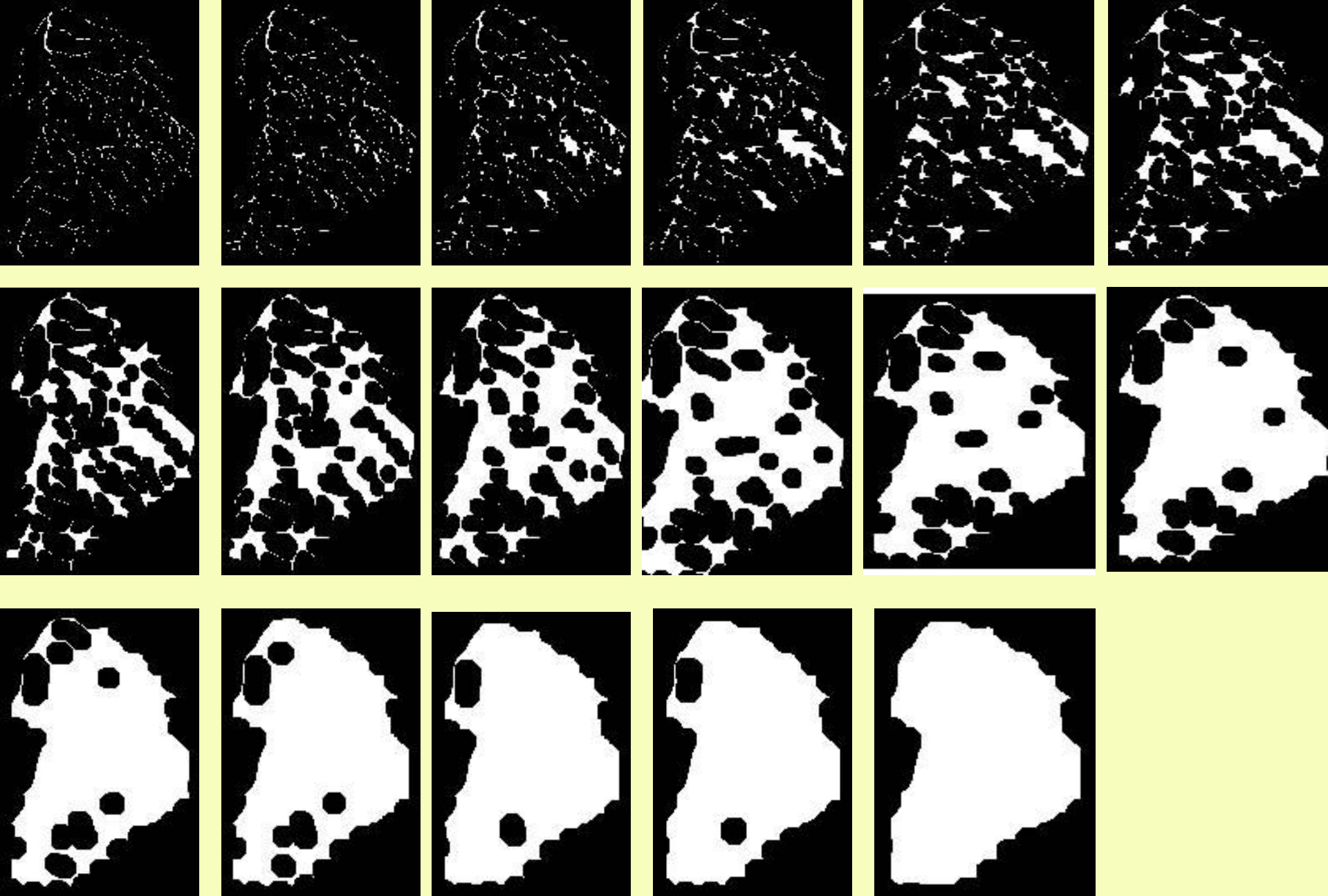
DEM of Gunung Ledang with 8 sub watershed partition



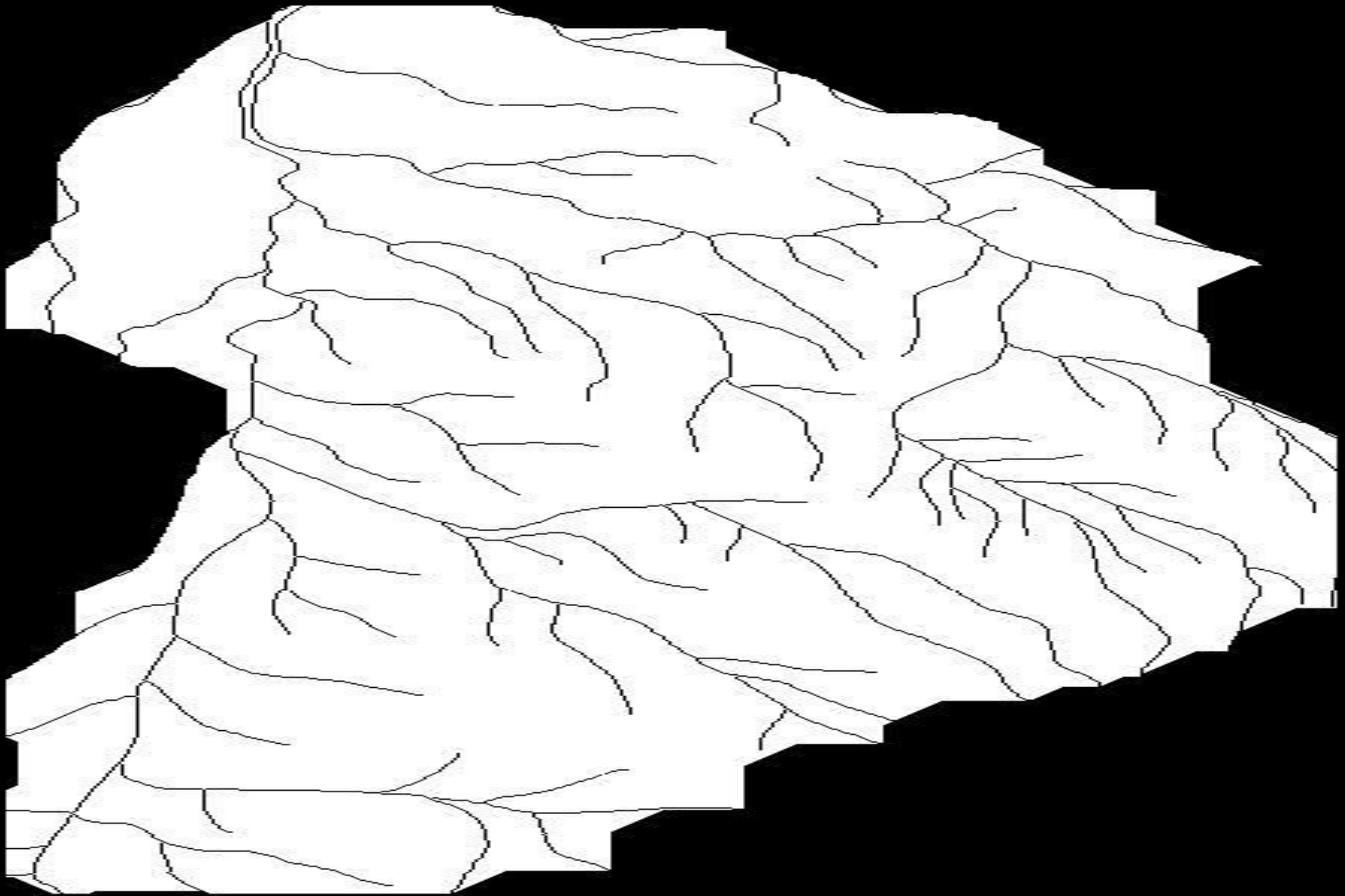
Channel network of sub basin 1



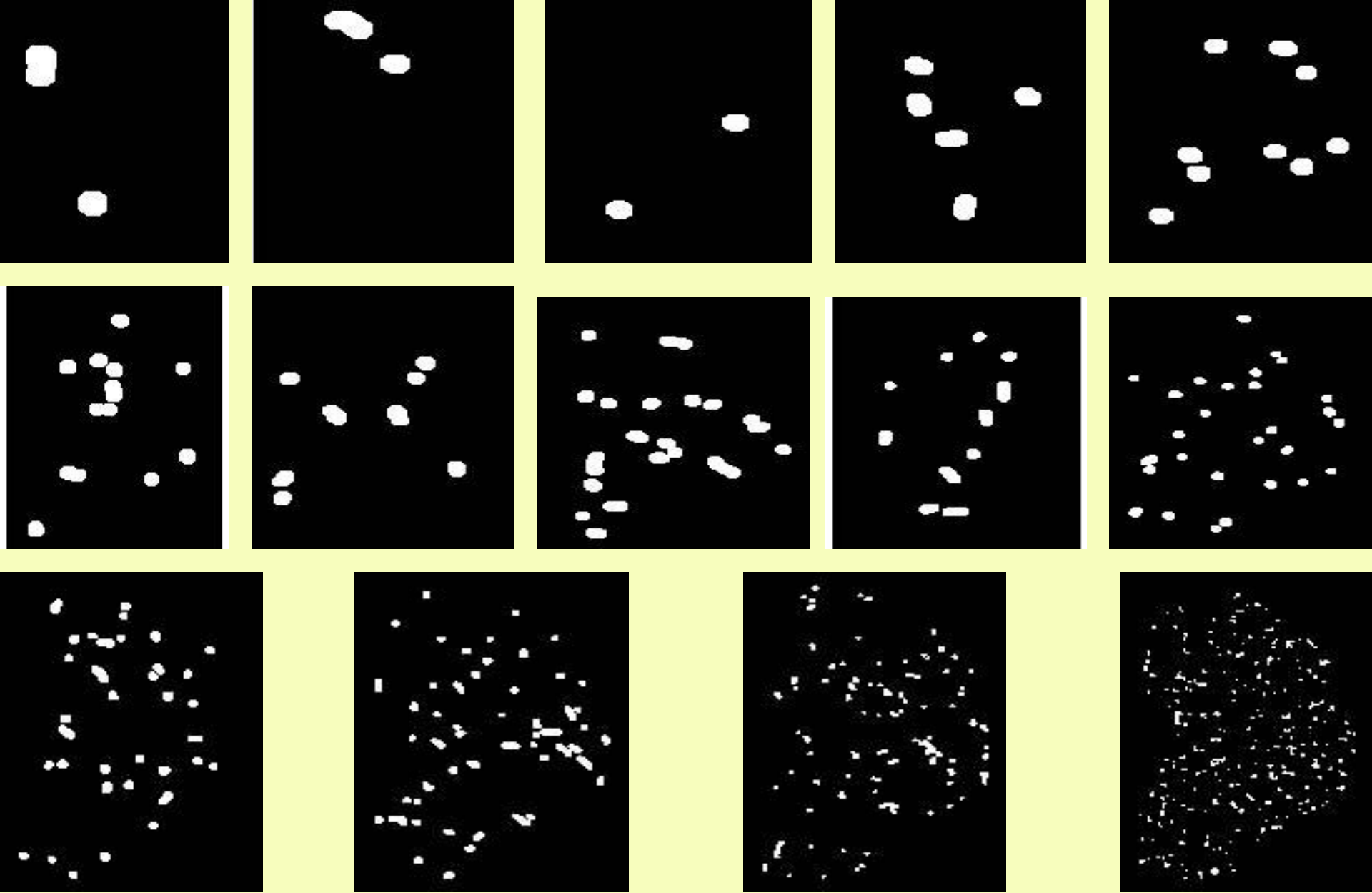
Iterative dilation of channel network of basin 1



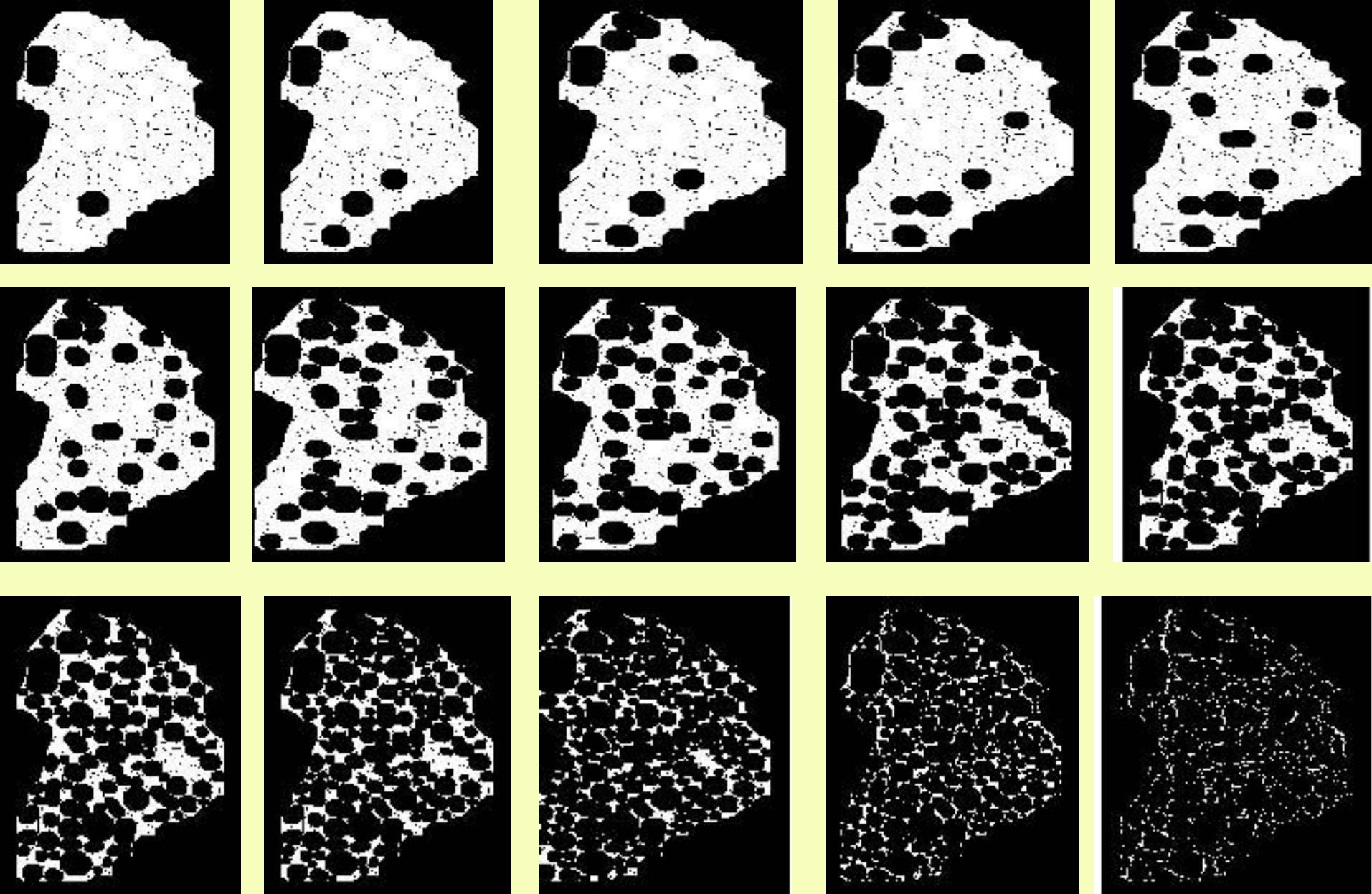
Iterative erosion applied to previous Fig



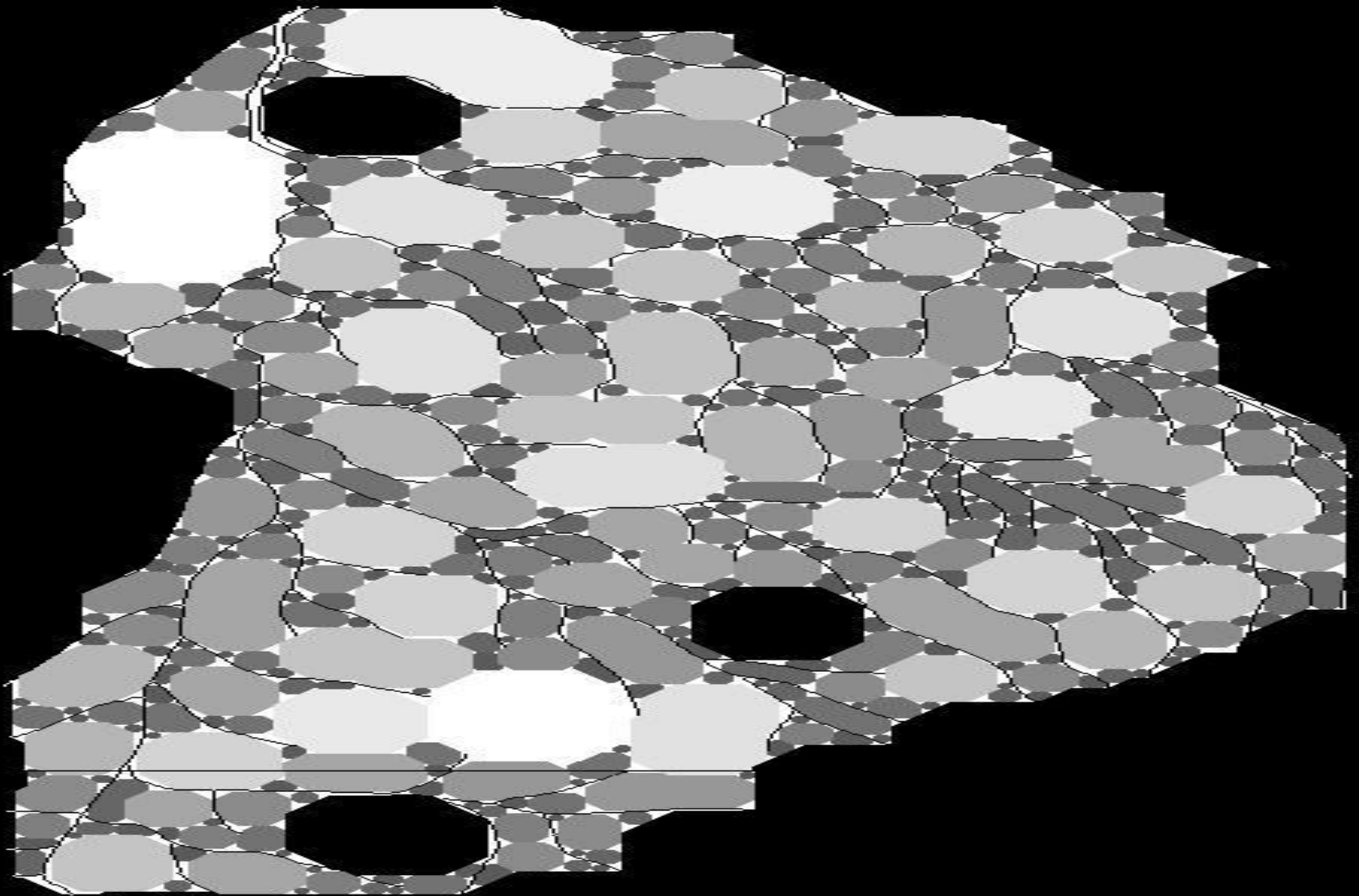
Non-network space of basin 1



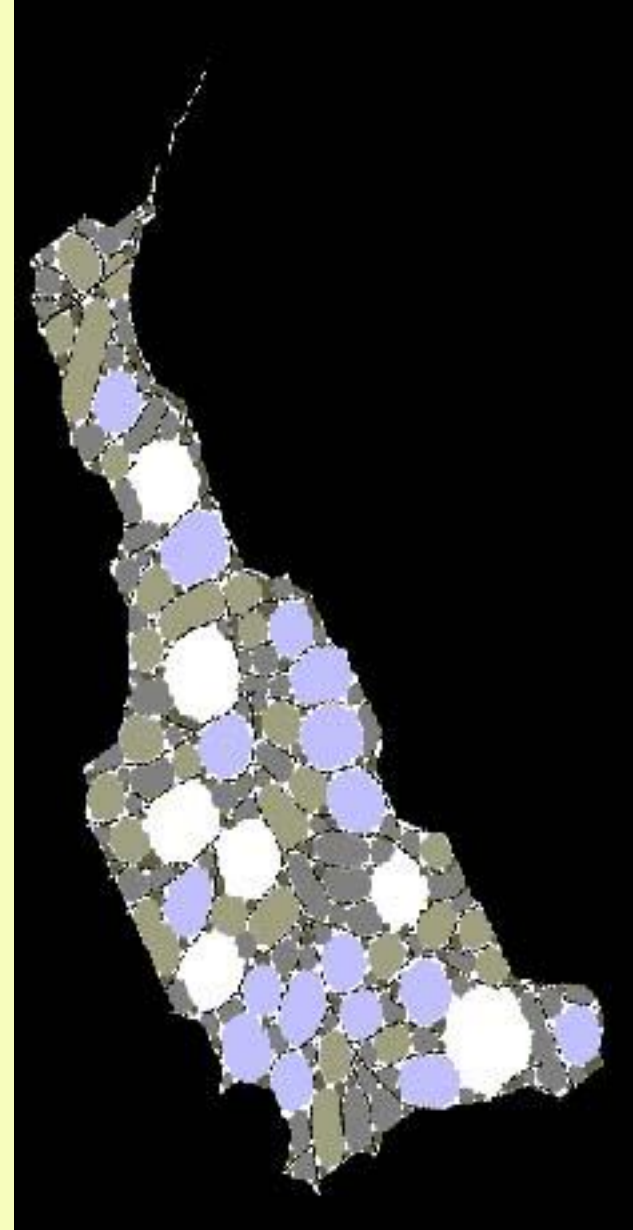
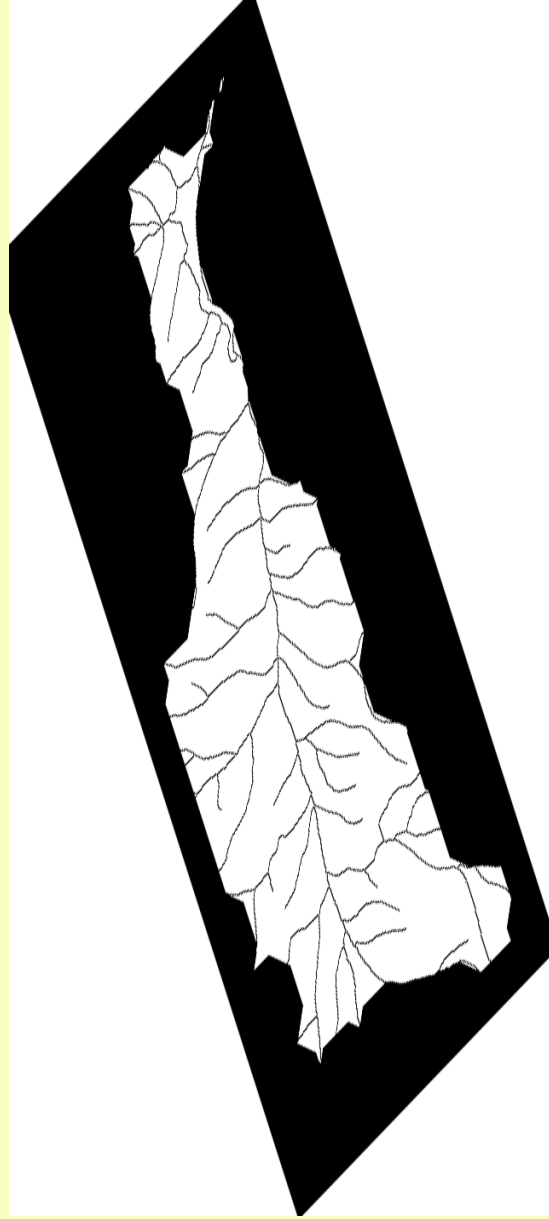
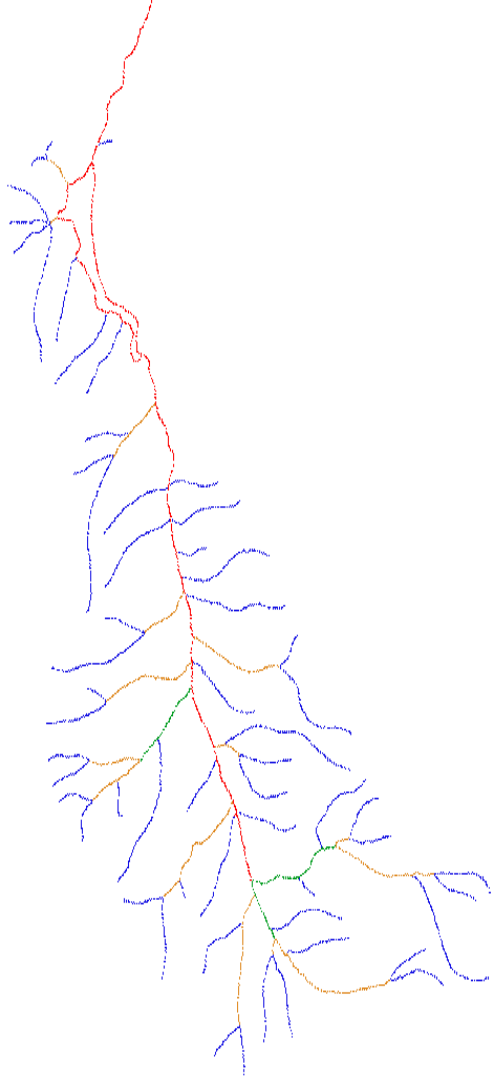
Iterative erosion applied to previous Fig.



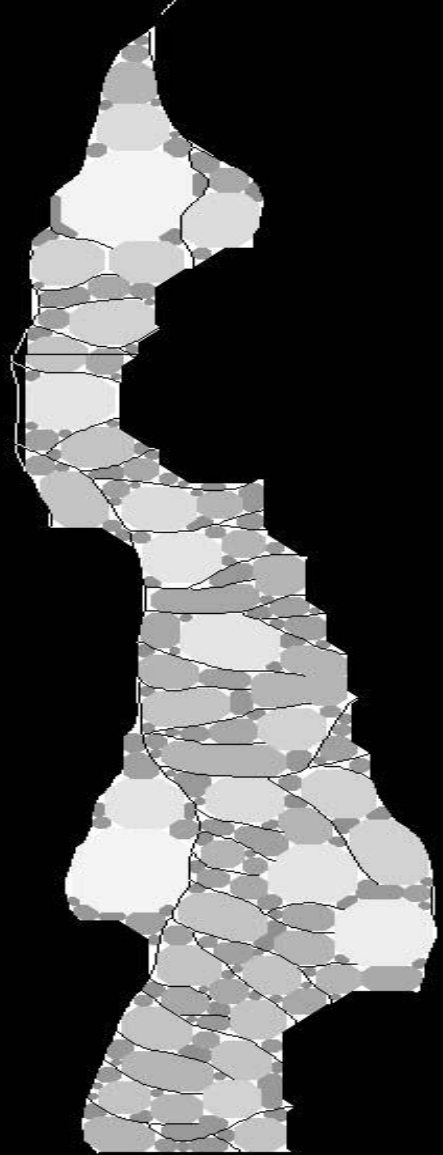
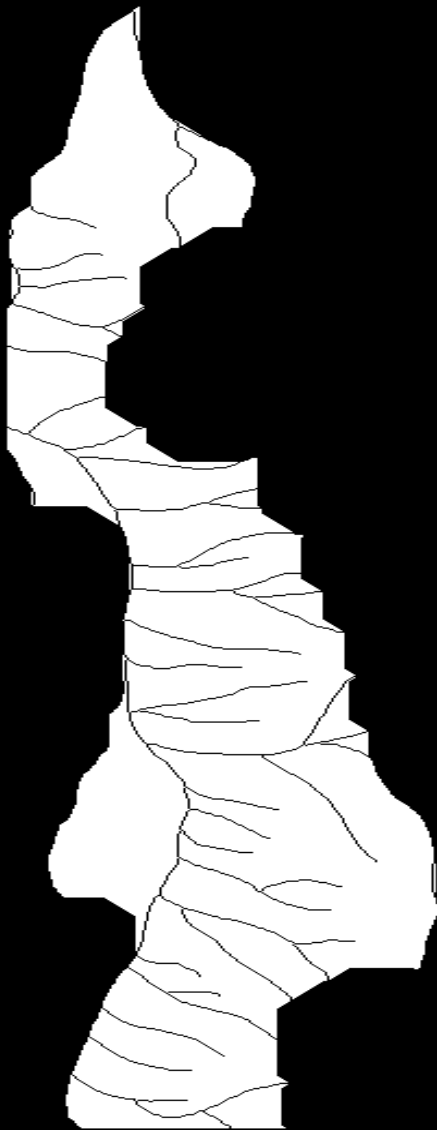
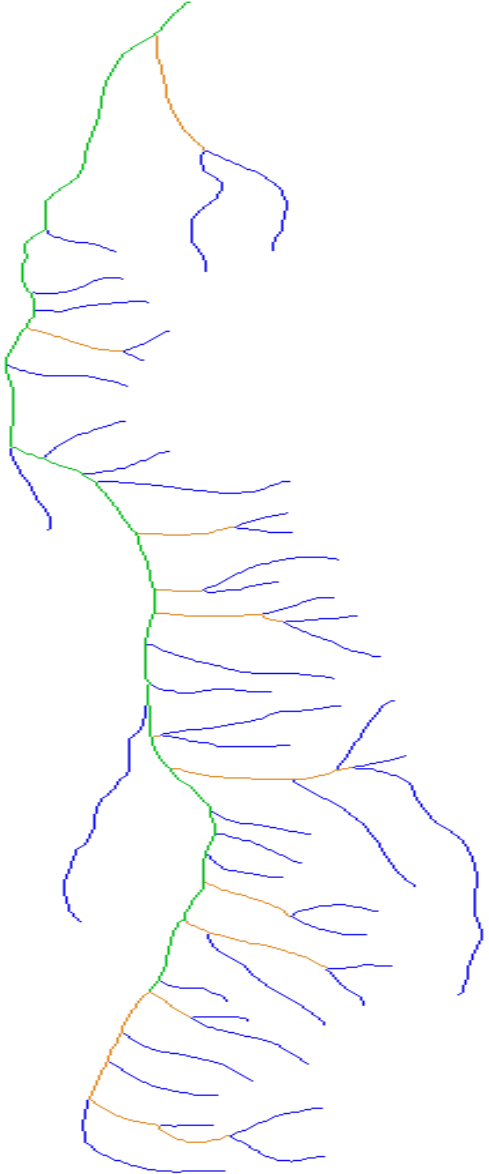
Iterative dilation applied to previous Fig.



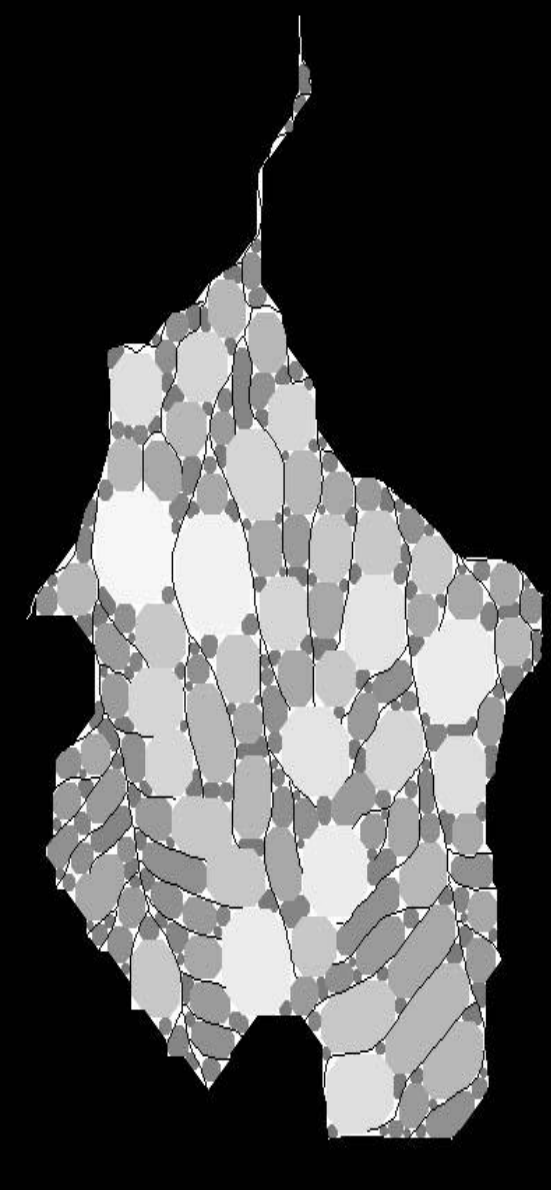
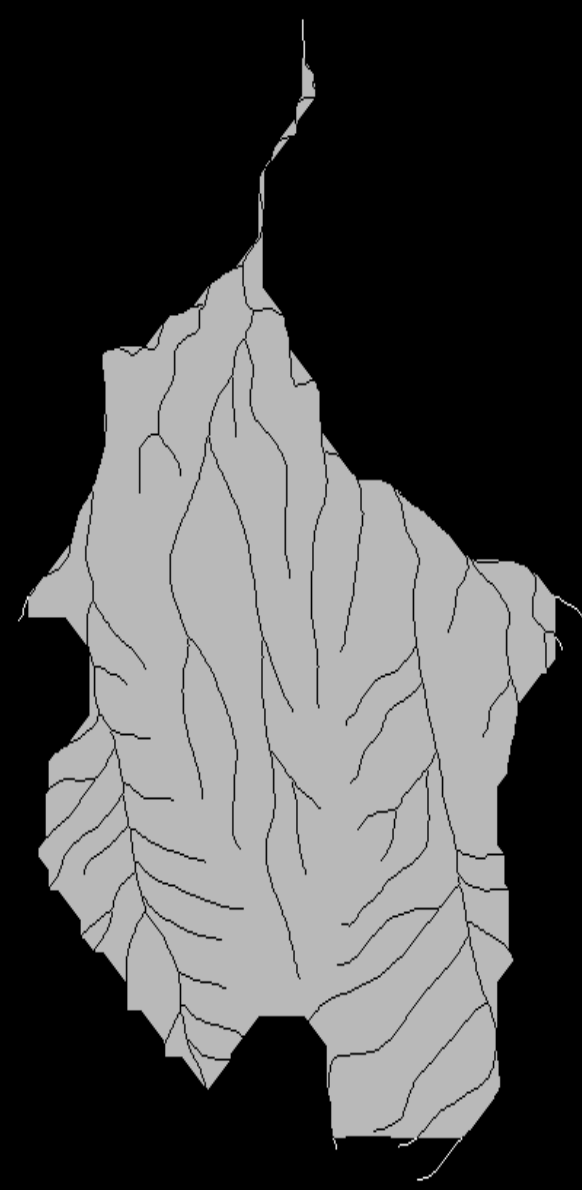
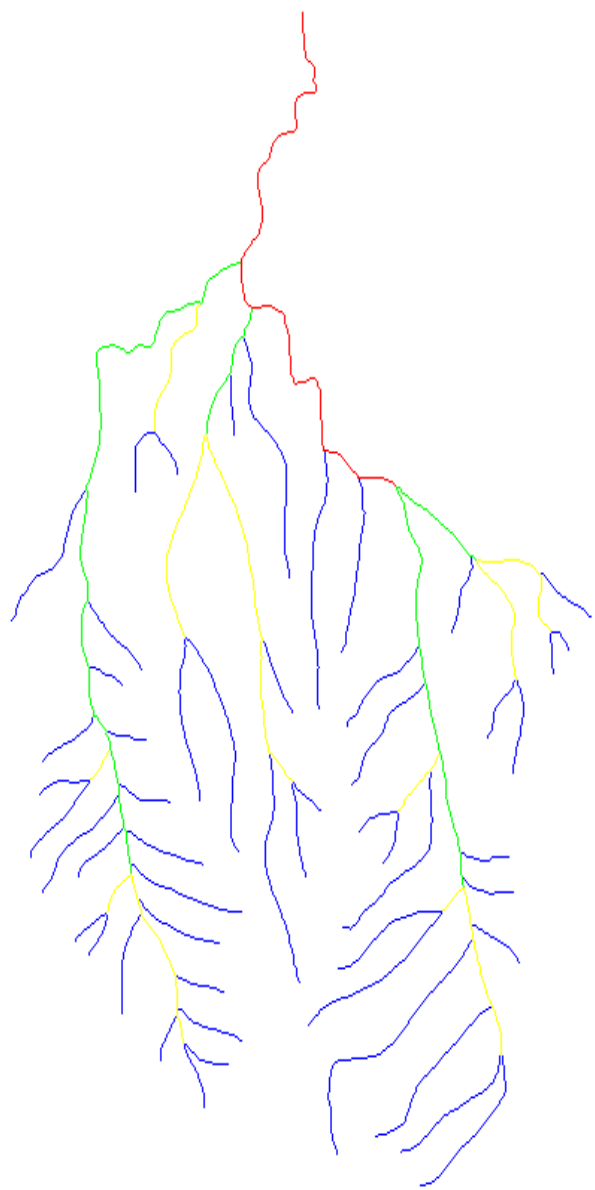
Decomposition of Non-network space in to non-overlapping disks of octagon shape of several sizes for basin 1 ³⁵



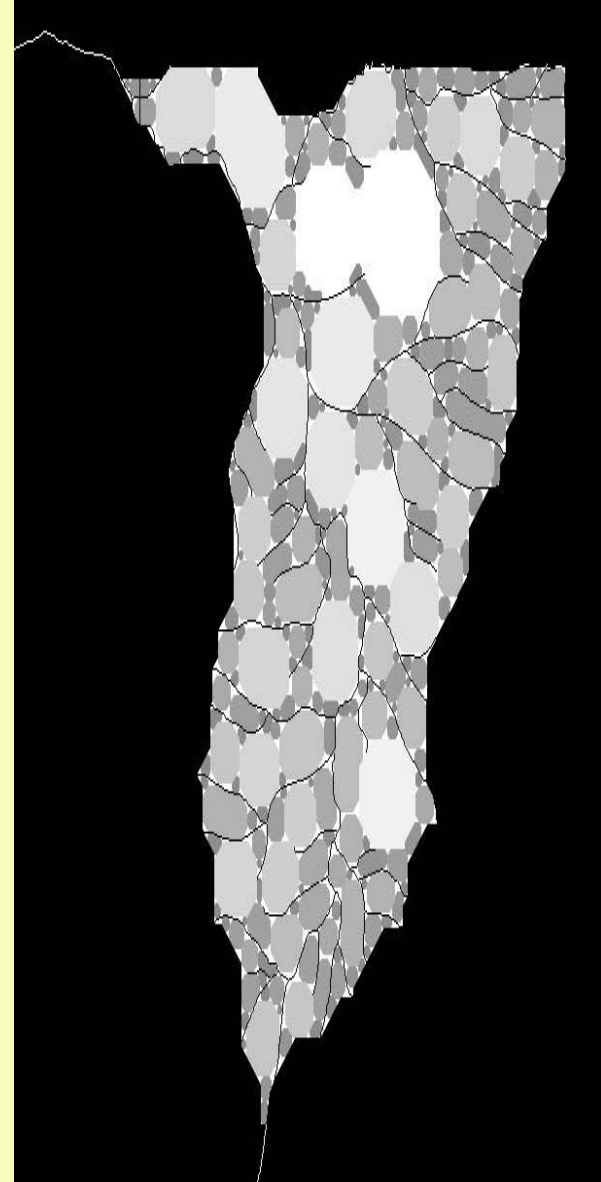
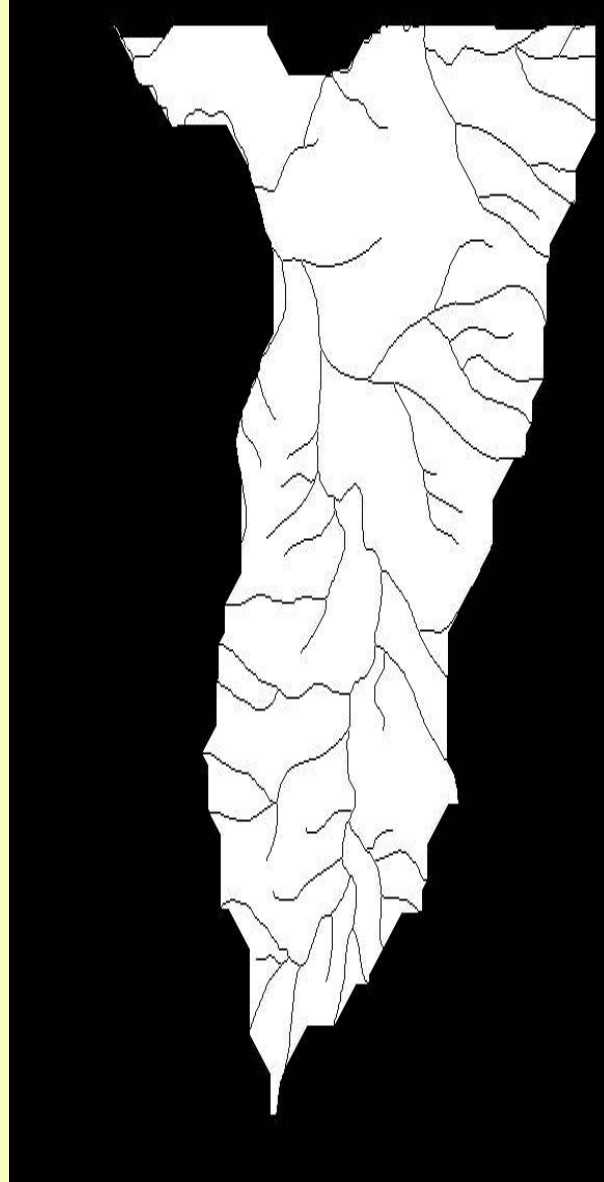
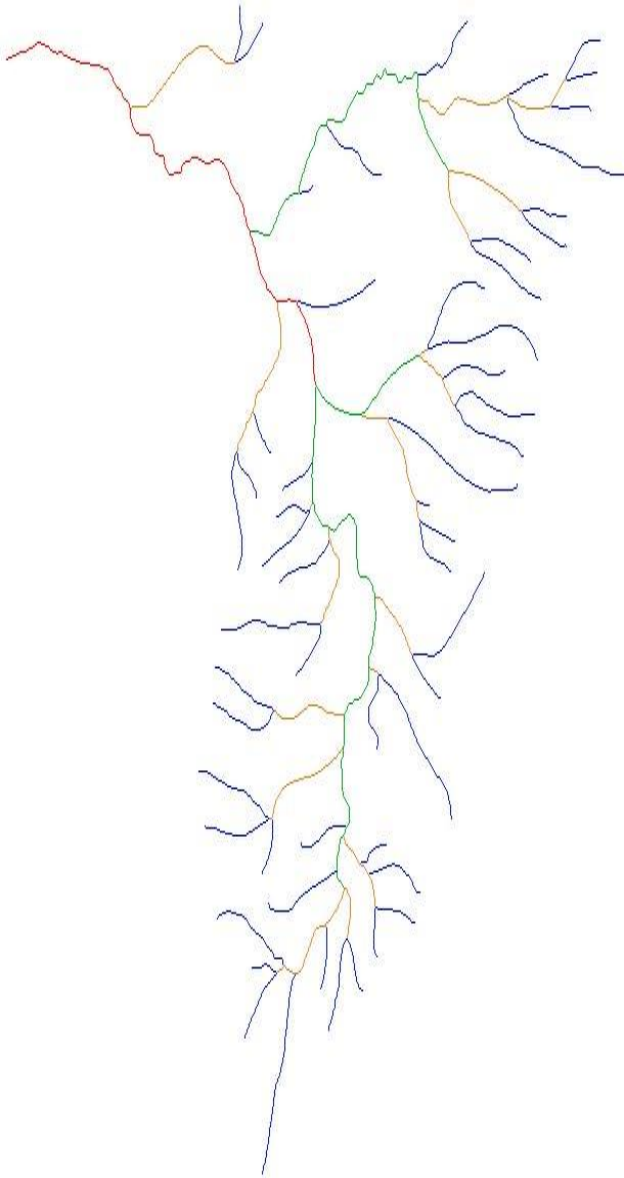
Sub basin 2



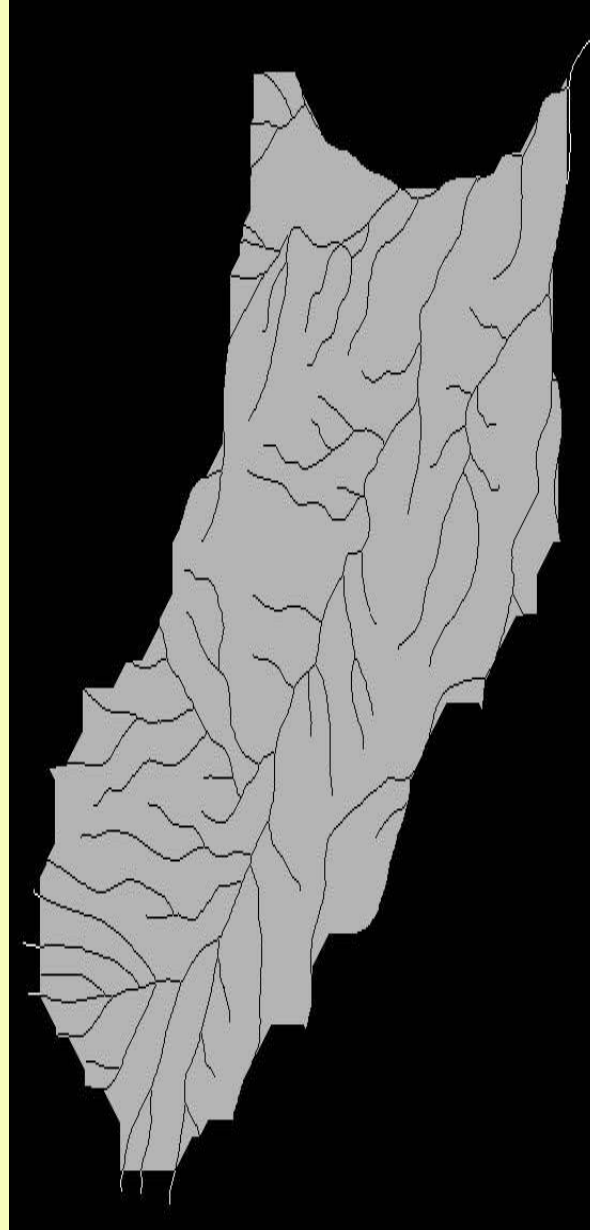
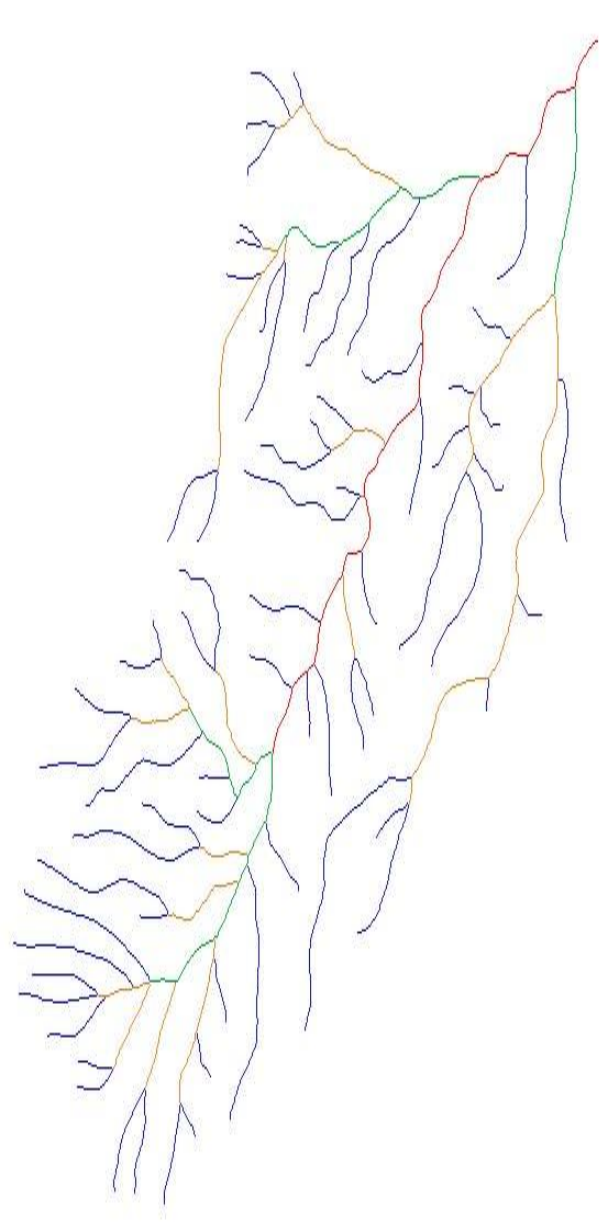
Sub basin 3



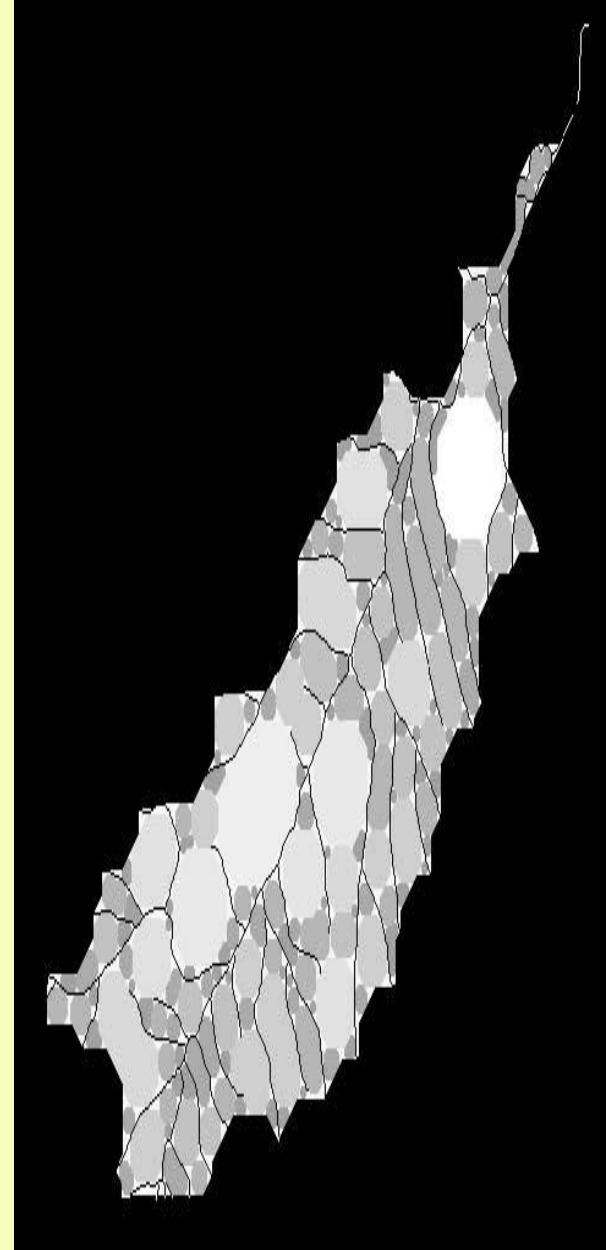
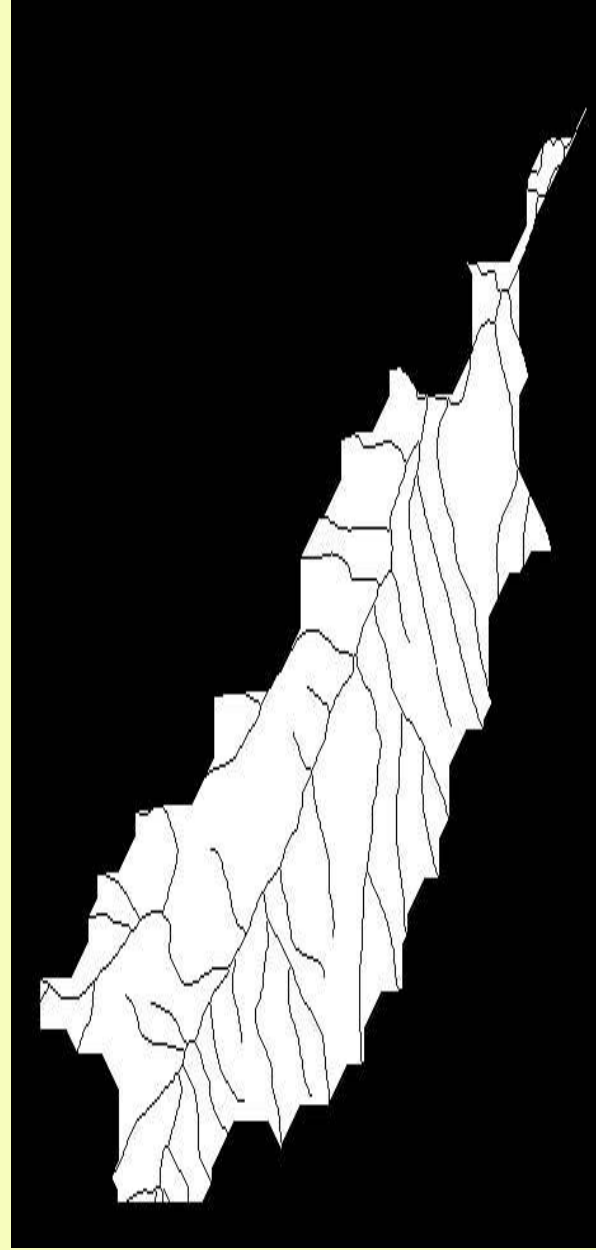
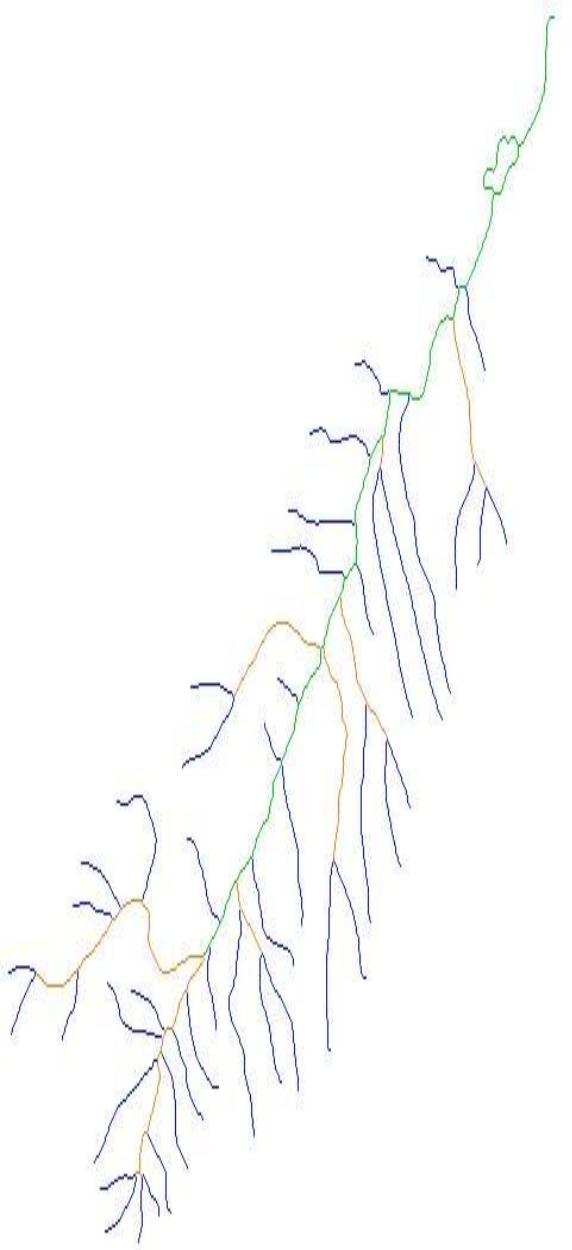
Sub basin 4



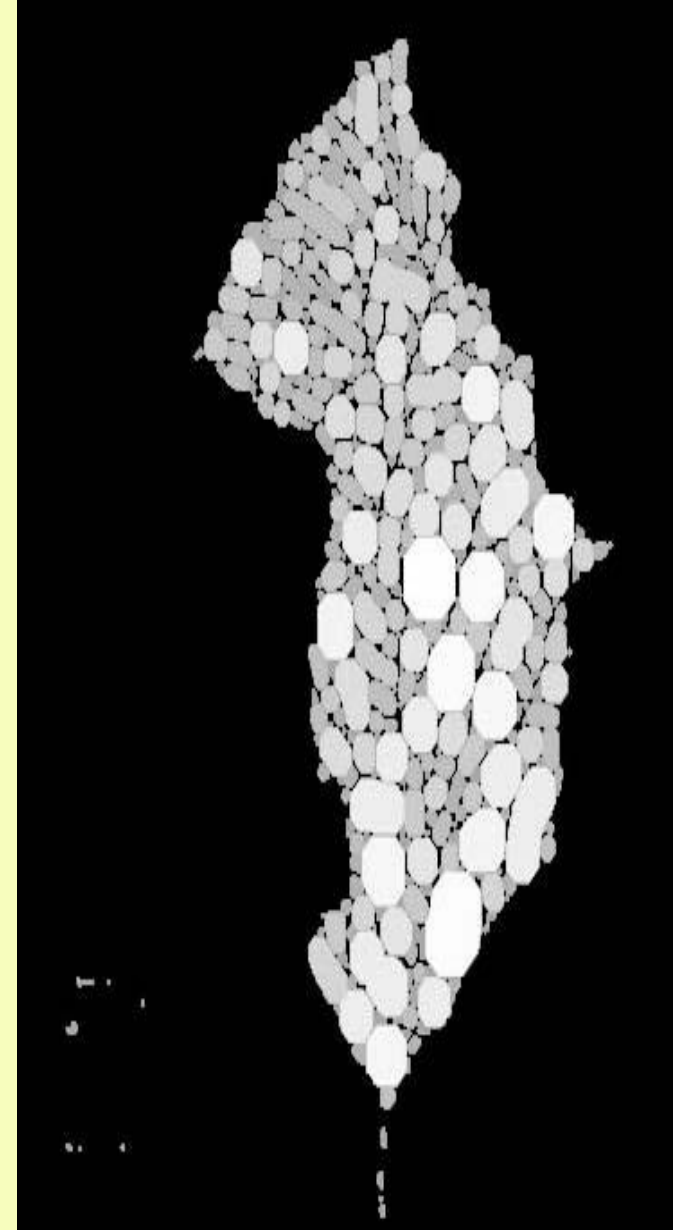
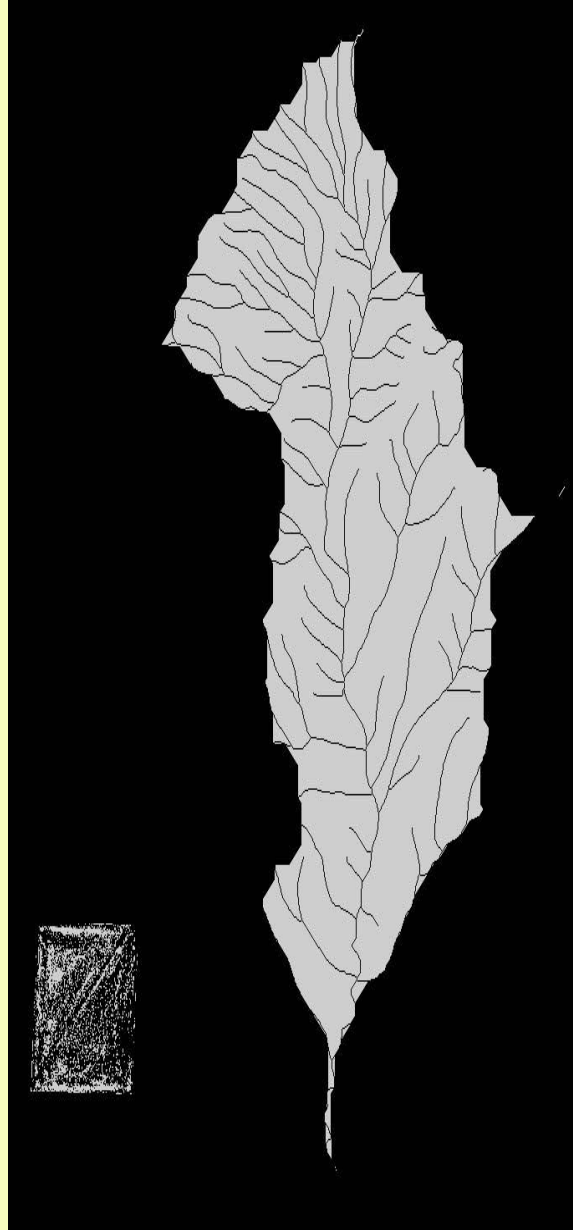
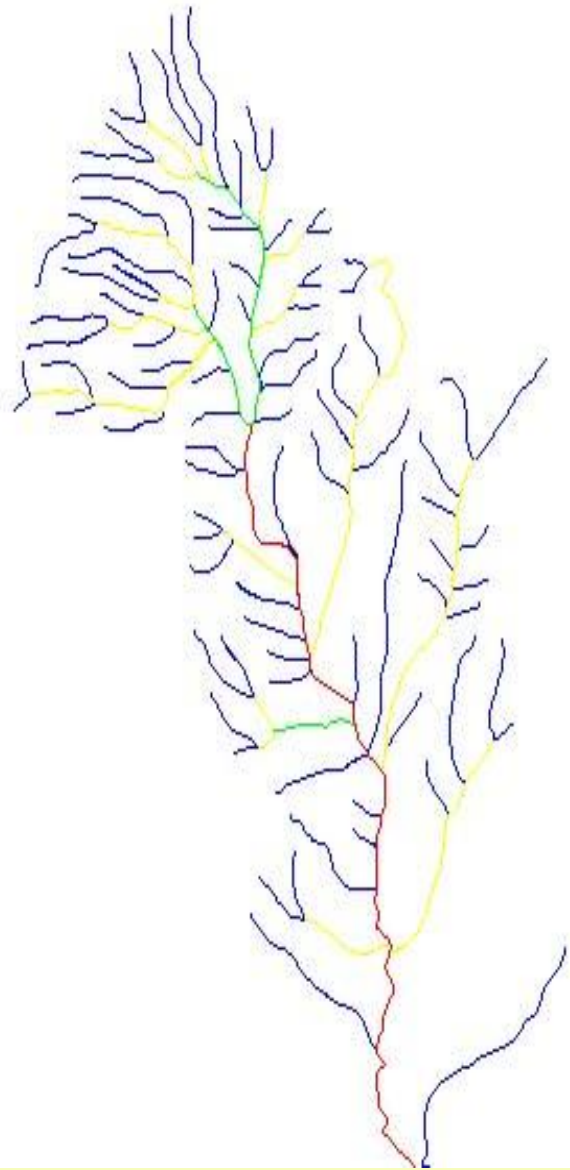
Sub basin 5



Sub basin 6



Sub basin 7



Sub basin 8

Basin No	Order Number				Stream length (in pixels)				R_B	R_L
	1	2	3	4	1	2	3	4		
1	85	18	4	2	4891	1611	551	849	3.45	1.90
2	58	15	3	1	2818	775	187	767	3.97	2.33
3	45	11	1	0	2346	594	770	0	6.64	3.87
4	53	11	4	1	2789	748	703	328	3.64	1.90
5	55	17	3	1	2834	961	659	374	3.96	2.07
6	70	18	4	1	3671	1182	518	431	4.16	2.01
7	46	8	1	0	2042	562	479	0	6.78	3.28
8	89	17	3	1	2477	809	194	294	4.57	2.09

Basic measures of networks of eight basins

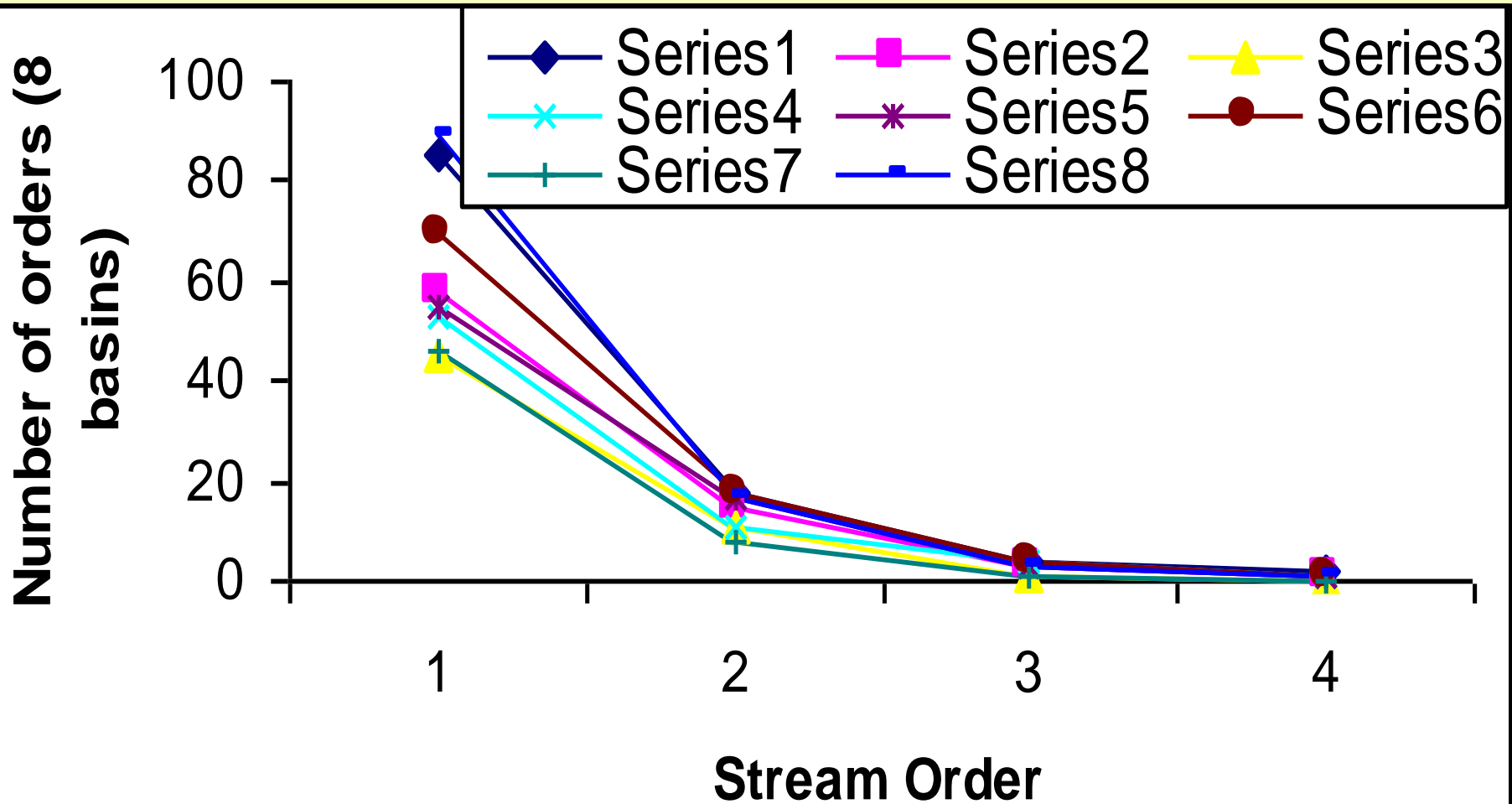
SE	Basin Number															
	1		2		3		4		5		6		7		8	
	N	A	N	A	N	A	N	A	N	A	N	A	N	A	N	A
34	-	-	-	-	-	-	-	-	316	10914 9	-	-	-	-	-	-
32	520	182014	-	-	-	-	-	-	168	10116 4	-	-	-	-	-	-
30	273	168813	-	-	-	-	-	-	118	93769	-	-	-	-	-	-
28	273	168813	28 2	84673	-	-	-	-	118	93769	-	-	-	-	-	-
26	273	168813	14 3	77373	203	68151	288	91357	77	81823	367	12578 2	-	-	440	13061 5
24	185	157455	93	70093	115	63288	152	83715	58	73992	200	11637 8	179	48876	243	12060 4
22	132	142011	93	70093	115	63288	104	77487	44	65496	144	10811 1	100	44098	162	10779 7
20	97	128123	70	63895	77	57872	77	68878	32	54786	96	94175	68	40018	106	89579
18	69	114338	52	55265	77	57872	58	61020	24	47302	65	80715	41	31764	70	74589
16	58	102690	33	42182	58	53641	40	50716	17	39672	52	72943	41	31764	46	58422
14	39	79374	24	35485	45	48404	28	39683	13	33652	34	58100	26	25760	34	49679
12	31	67158	17	27707	31	38240	17	28488	10	27837	22	45704	13	17946	22	37938
10	20	48742	10	19564	19	28316	10	20138	8	23638	17	40300	9	13669	11	21426
8	11	32274	7	14762	12	20895	7	15941	6	19163	14	36029	5	9833	8	16888
6	6	18356	4	9486	8	16249	5	12226	4	12004	10	28786	4	8888	4	10145
4	4	14019	2	5784	3	8794	2	5587	2	6088	6	16009	2	5435	2	6078
2	2	5859	1	3339	2	6711	1	2753	1	2407	2	5978	1	2360	1	2632

Number & corresponding contributing areas of non-overlapping disks of various sizes decomposed from non-network space of 8 basins

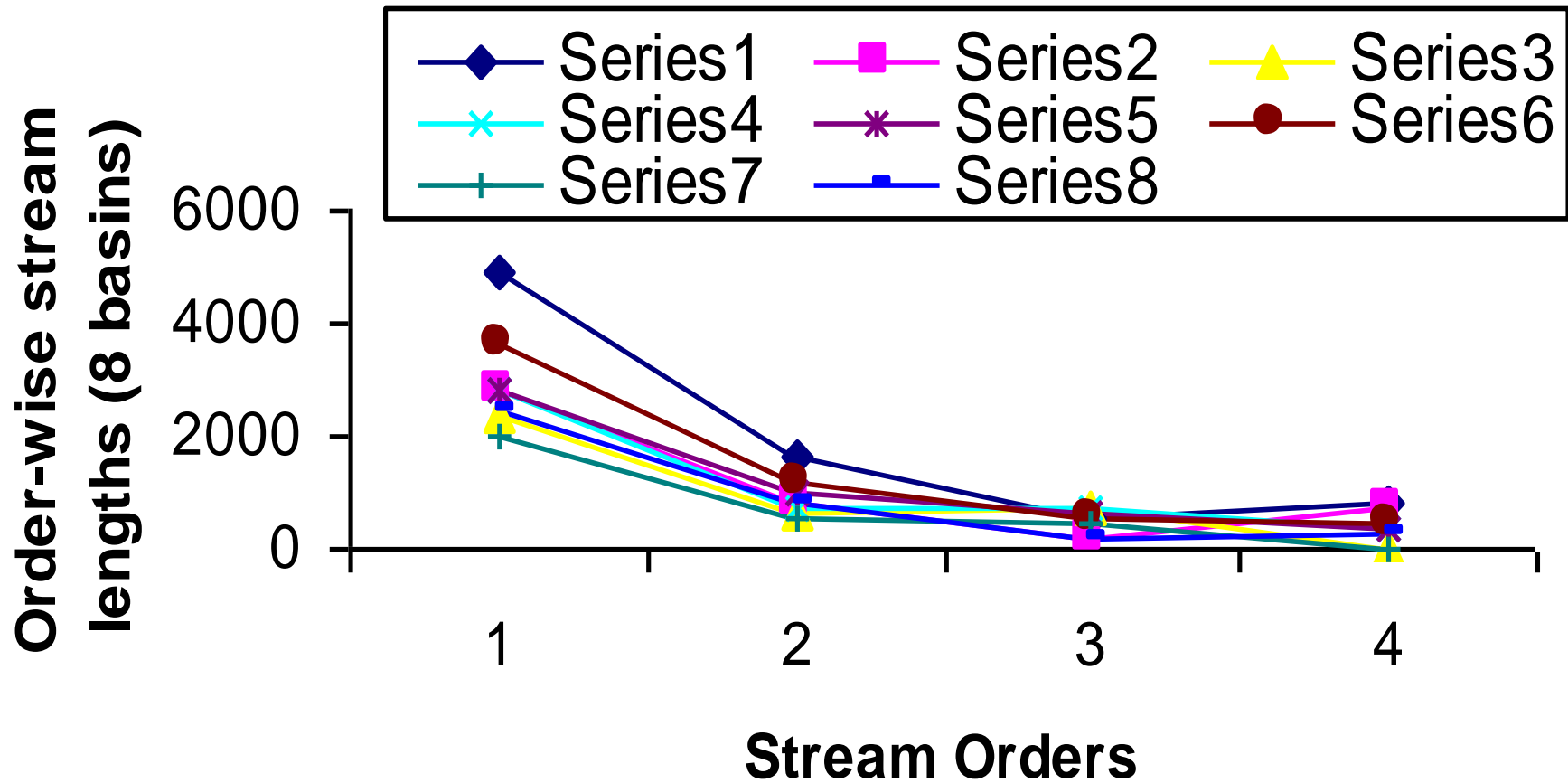
Dimensions derived from morphometry of network and non network space

Basin Number	Network FD ($\text{Log } R_B / \text{Log } R_L$)		R vs A	R vs N	A vs N
1	1.83	193	1.34	2.04	1.50
2	0.86	1.63	1.33	1.23	1.59
3	0.98	1.41	1.02	1.87	1.80
4	2.07	2.01	1.43	2.17	1.52
5	1.73	1.90	1.34	1.94	1.43
6	1.84	2.04	1.13	1.87	1.63
7	1.33	1.61	1.23	2.08	1.70
8	1.65	2.06	1.61	2.38	1.49

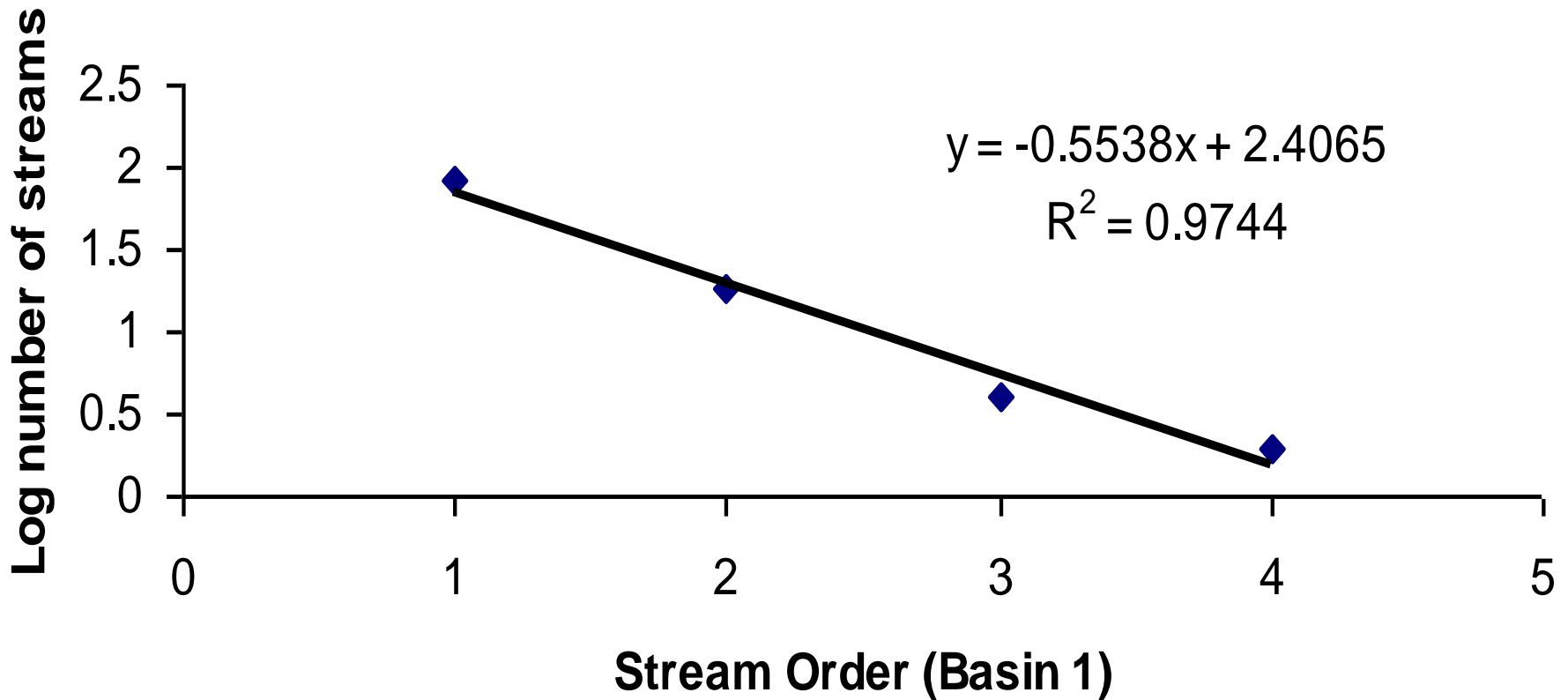
Graphical plot between stream order and order-wise stream number



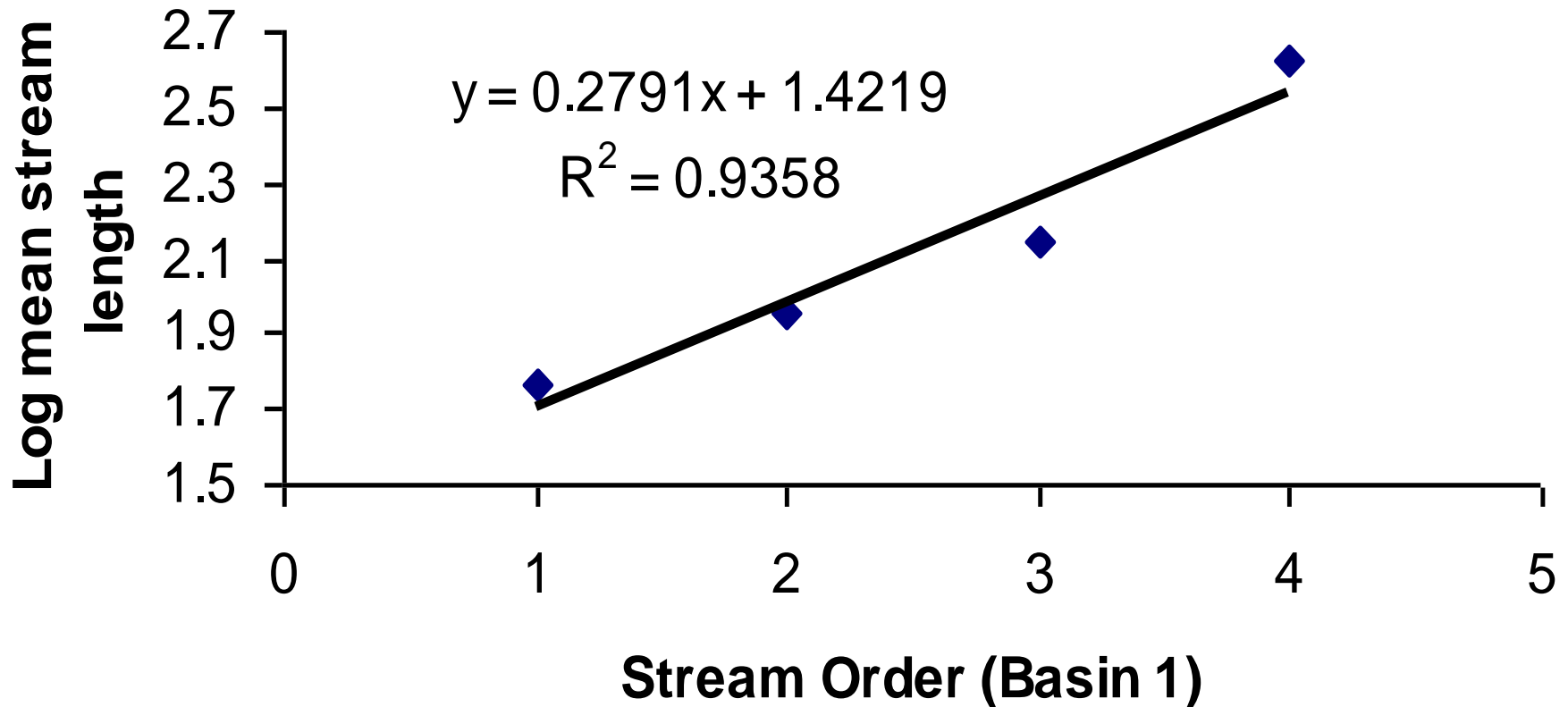
Graphical plot between stream order and order-wise stream lengths



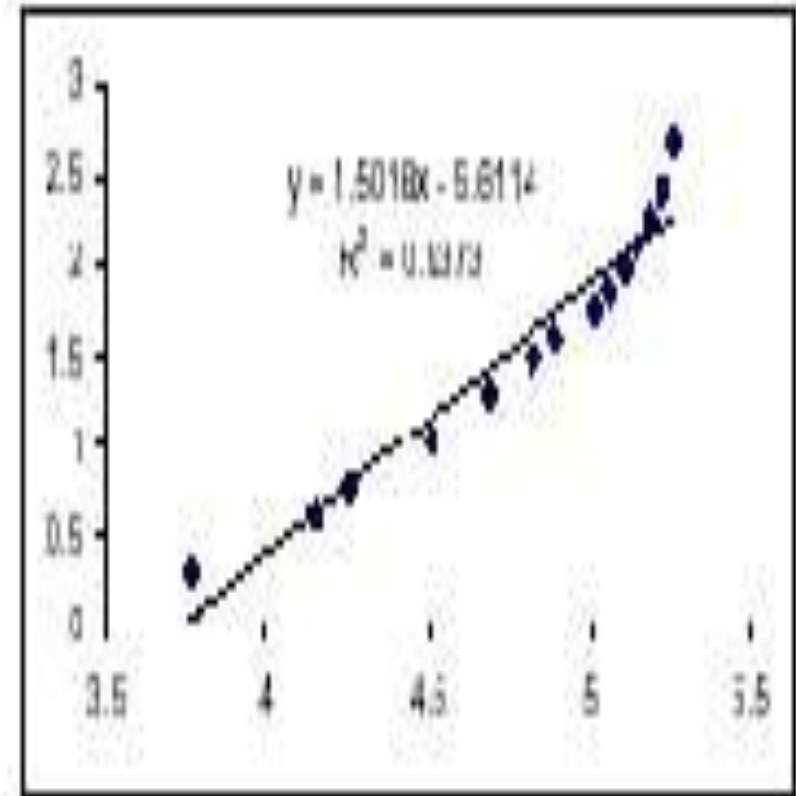
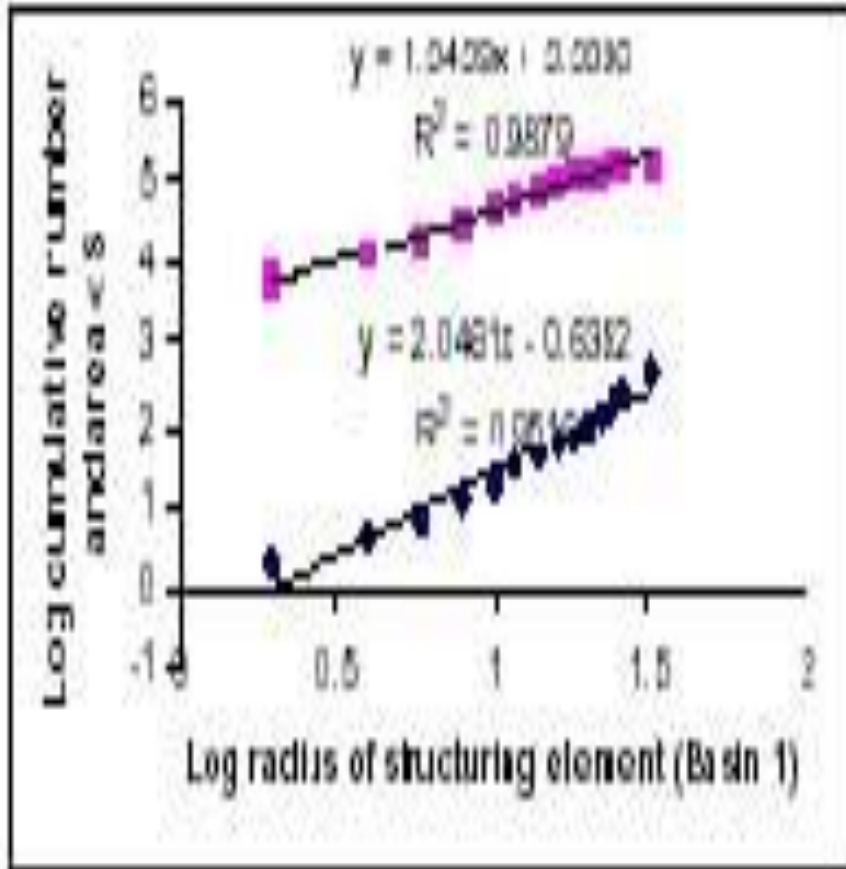
Graphical plot between stream order versus logarithm of order-wise numbers for basin 1



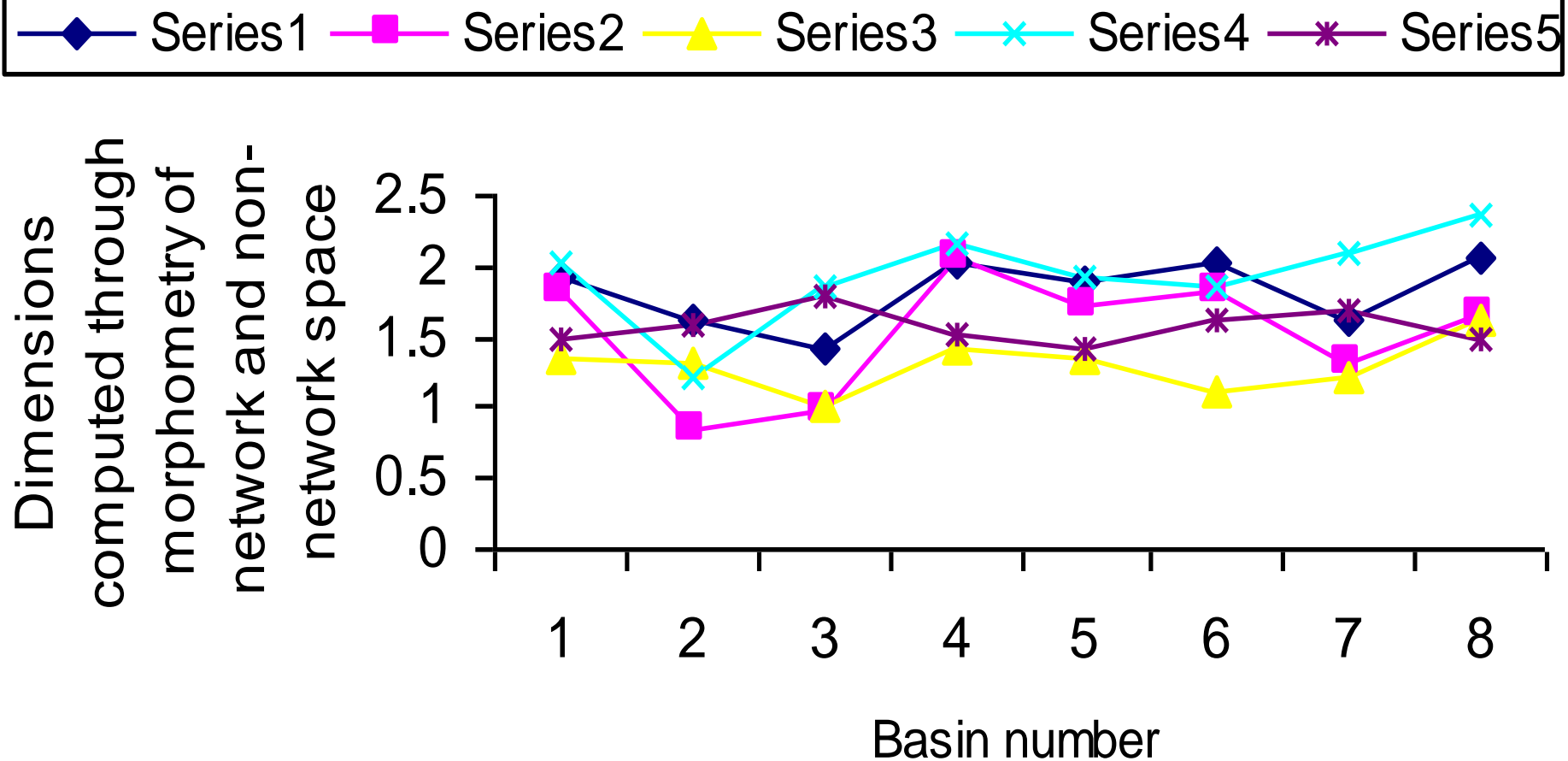
Graphical plot between stream order versus order-wise mean stream lengths for basin 1

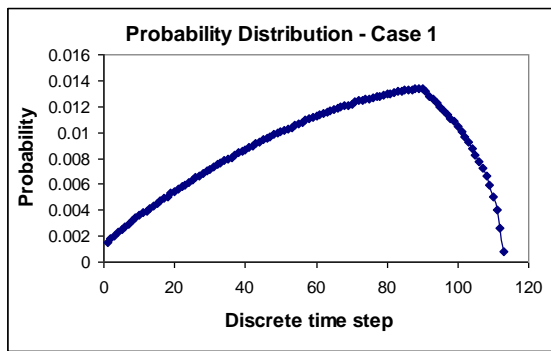


Morphometric parameter computations achieved through decomposition of non-network space

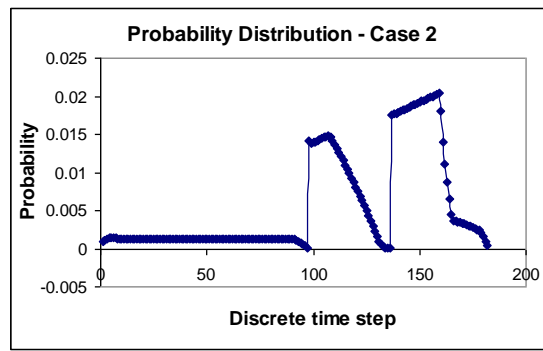


Basin number versus varied dimensions derived from morphometry of networks and non-network spaces

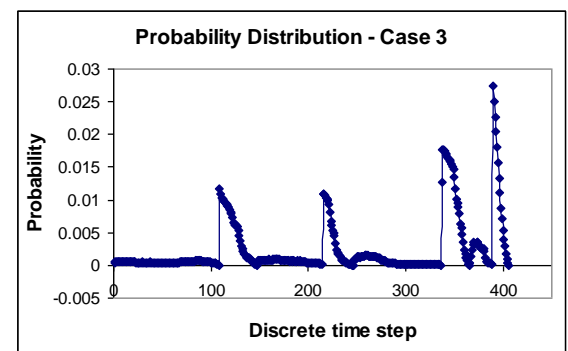




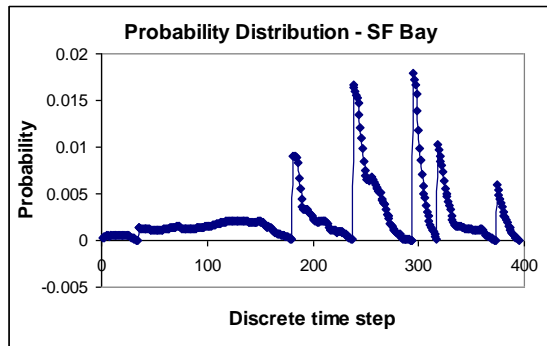
(a)



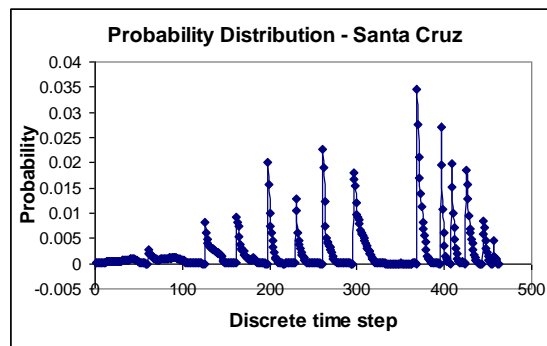
(b)



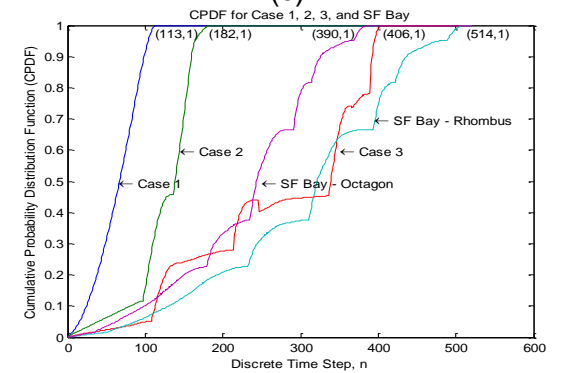
(c)



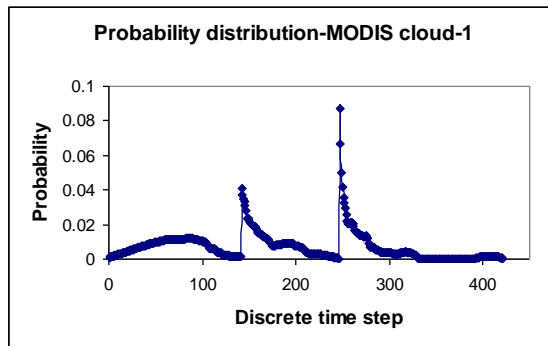
(d)



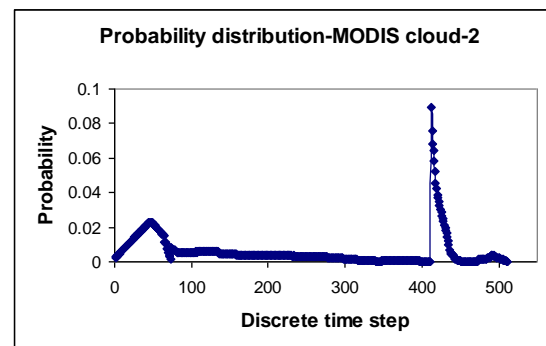
(e)



(f)



(g)



(h)

Figure. Probability of estimated area flooded/propagated at each discrete time step.

VISUALIZATION OF UNIQUE MORPHOLOGICAL FEATURES

Visualization of rock porous medium, pore channel, pore throats, and pore bodies

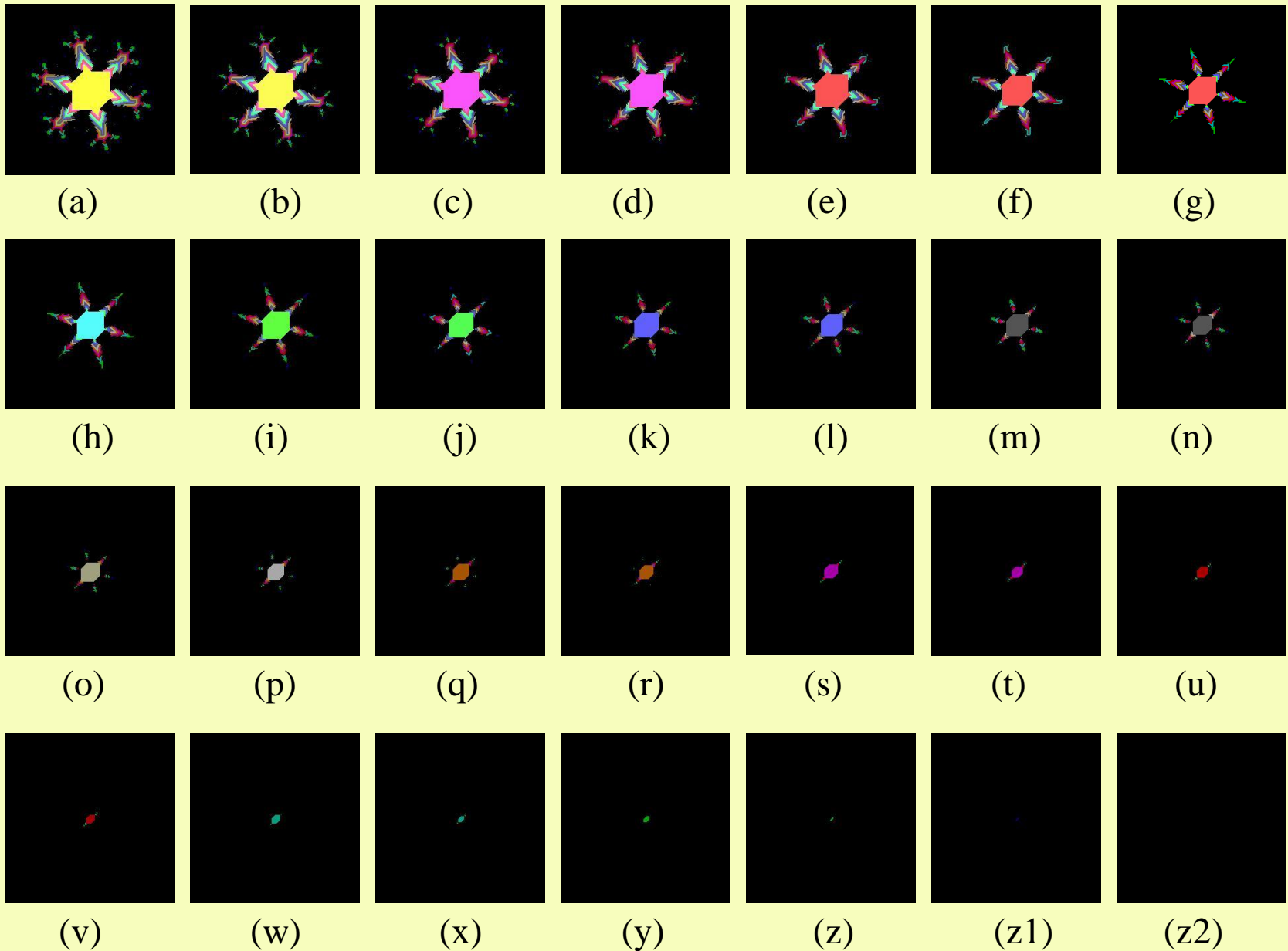


Figure : Extracting pore throat from eroded **triadic Koch curve** images by structuring element of octagon.

Top and side views of 3D
model at

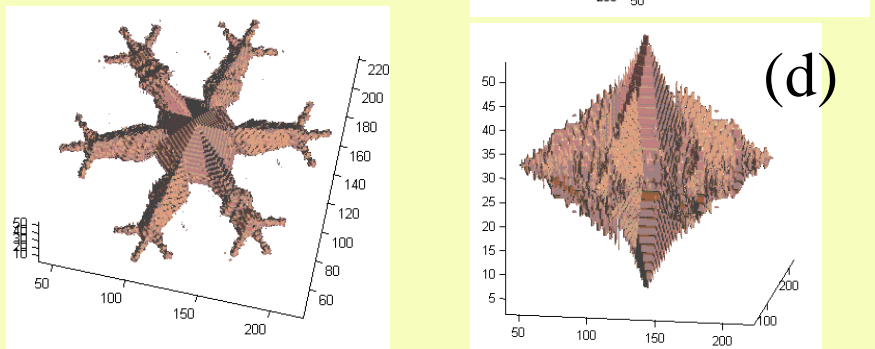
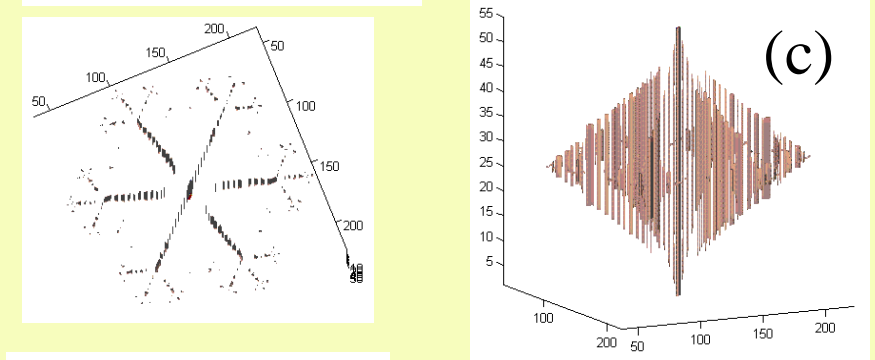
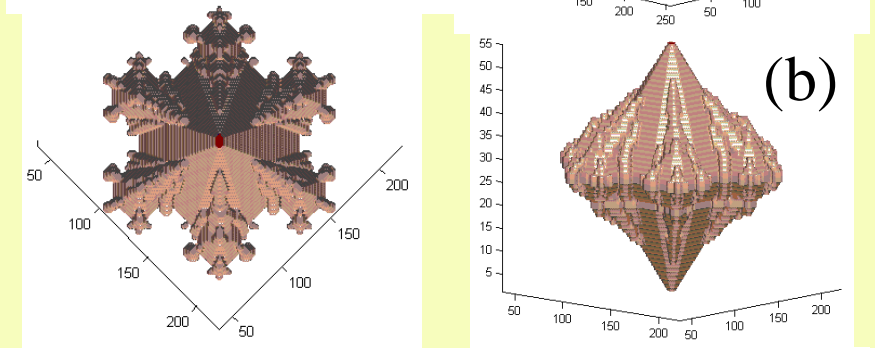
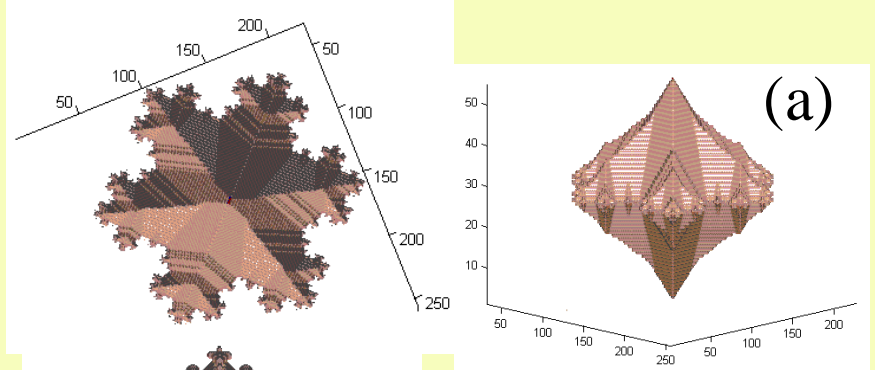
(a) binary pore,

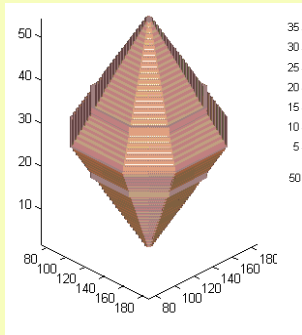
(b) pore-bodies,

(c) pore-channel, and

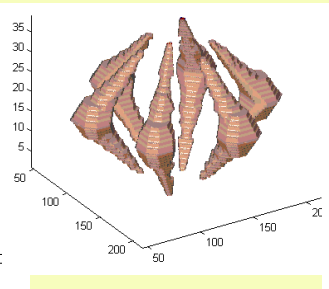
(d) pore-throat

of **triadic Koch curve**

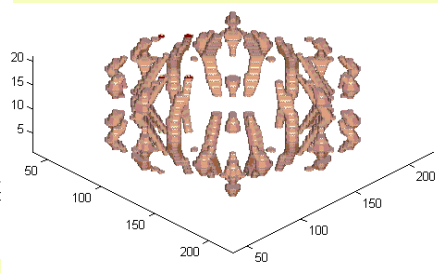




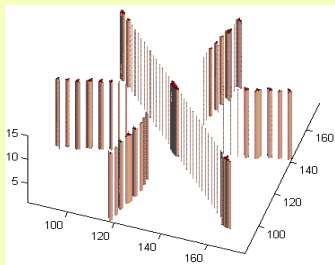
(a)(i)



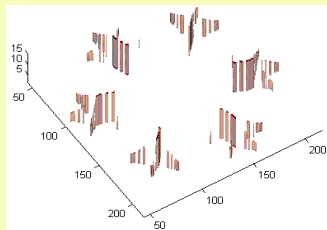
(a)(ii)



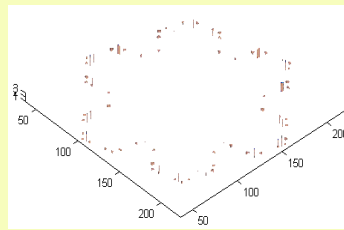
(a)(iii)



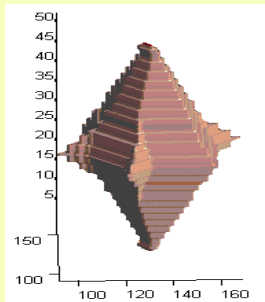
(b)(i)



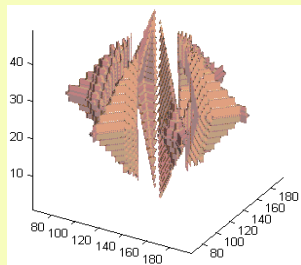
(b)(ii)



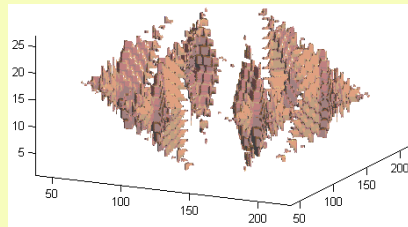
(b)(iii)



(c)(i)



(c)(ii)



(c)(iii)

The diagram shows the order-wise isolated 3D pore quantities at (i) inner, (ii) middle and (iii) outer layers of

(a) pore bodies,

(b) pore channels, and

(c) pore throats.

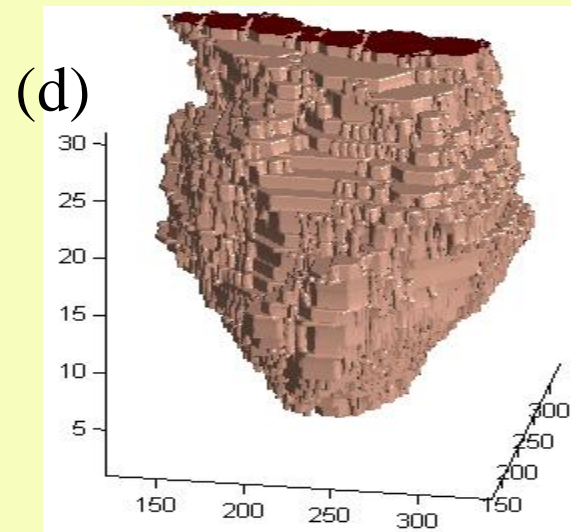
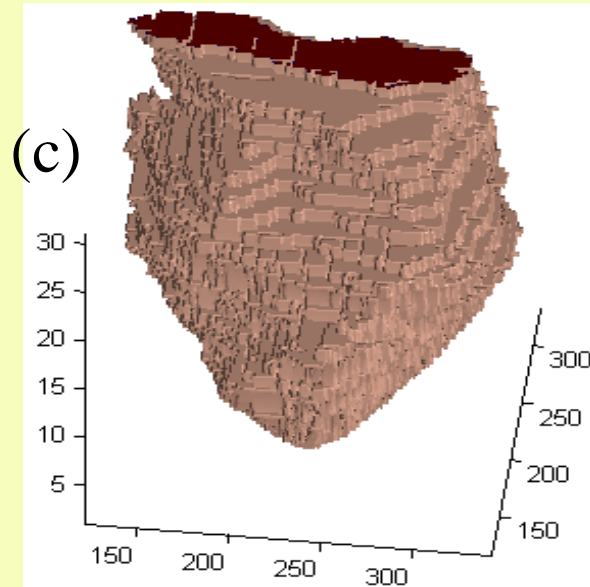
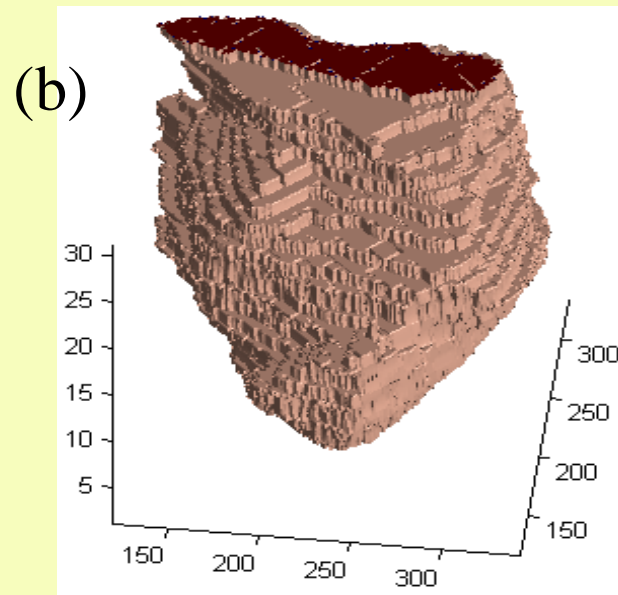
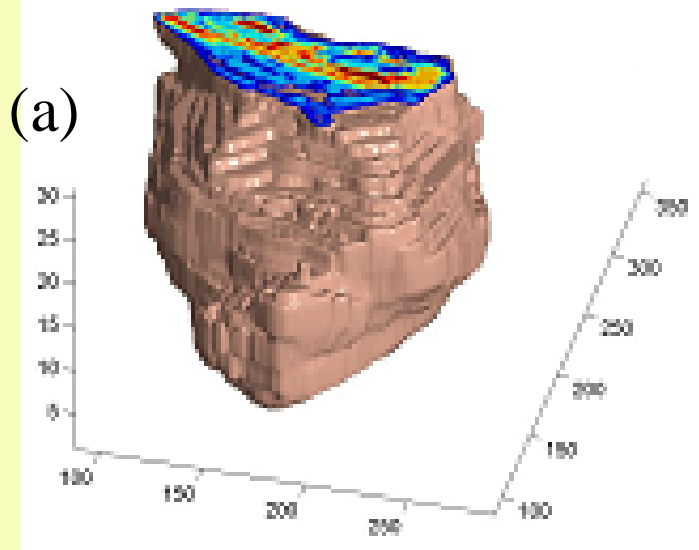


(a)

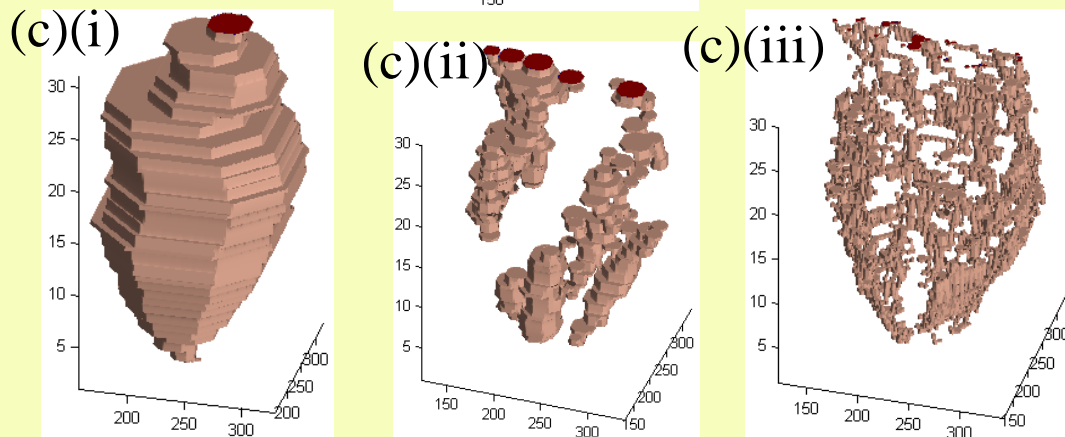
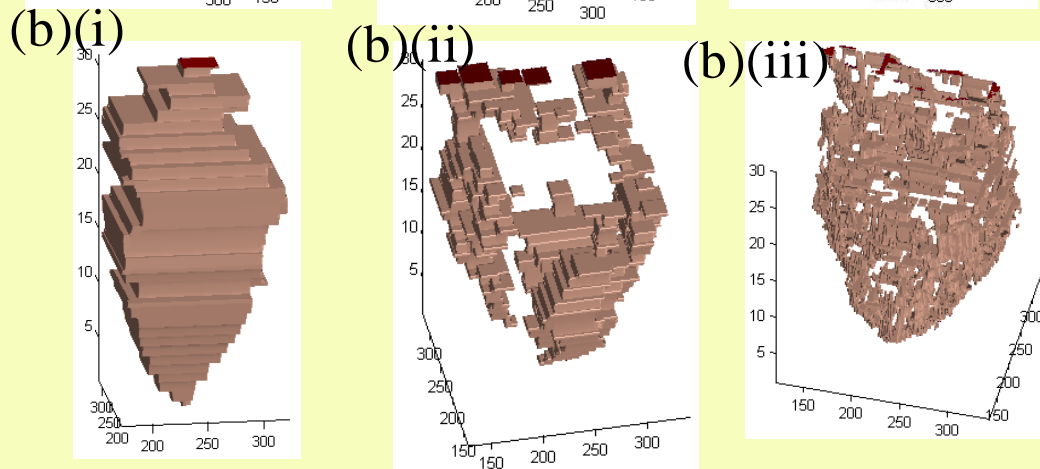
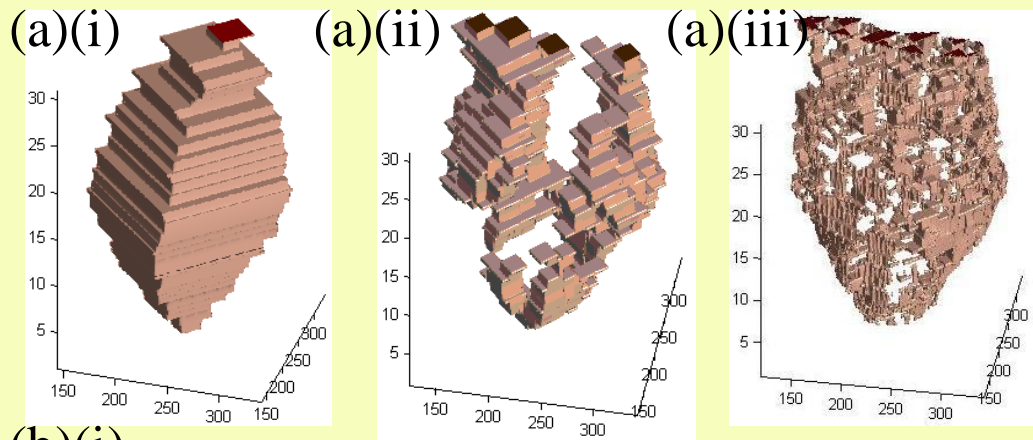


(b)

(a) The photograph of schist rock sample; (b) the CT scans applied at schist rock sample



The 3D reconstruction of (a) binary schist image; non-overlapping decomposition technique by structuring elements of (b) rhombus, (c) square and (d) octagon



Order-wise isolated 3D rock quantities at (i) inner, (ii) middle and (iii) outer layers rock by structuring elements

(a) rhombus

(b) square, and

(c) octagon.

Conclusions

1. Various Computational geophysics related topics are dealt with.

(a) In modeling geophysical phenomena, application of mathematical morphology is relatively less employed. I have addressed several interesting problems by studying the basin via mathematical morphology.

◆ In particular, digital image processing techniques , geo statistical tools and geo computational techniques that are relatively less employed to deal with catchment characterization studies are applied in this investigation.

2. These techniques are proved to be robust in deriving complex topological and surficial features of geophysical significance.

Acknowledgments: Grateful to collaborators, mentors, reviewers, examiners, and doctoral students—Prof. S. V. L. N. Rao, Prof. B. S. P. Rao, Dr. M. Venu, Mr. Gandhi, Dr. Srinivas, Dr. Radhakrishnan, Dr. Lea Tien Tay, Dr. Chockalingam, Dr. Lim Sin Liang, Dr. Teo Lay Lian, Prof. Jean Serra, Prof. Gabor Korvin, Prof. Arthur Cracknell, Prof. Deekshatulu, Prof. Philippos Pomonis, Prof. Peter Atkinson, Prof. Hien-Teik Chuah and several others.